MOLECULAR GENETICS OF THE IMMOTILE SHORT TAIL SPERM DEFECT

by

Anu Sironen

From the Department of Physiology, Institute of Biomedicine, University of Turku, Turku, Finland and MTT Agrifood Research Finland, Biotechnology and Food Research, Animal Genomics, Jokioinen, Finland

Supervised by

Professor Jorma Toppari, MD, Ph.D.
Department of Physiology
Institute of Biomedicine
Faculty of Medicine
University of Turku
Turku, Finland

and

Docent Johanna Vilkki, Ph.D.
Agrifood Research Finland MTT
Biotechnology and Food Research
Animal Genomics
Jokioinen, Finland

Reviewed by

Professor Hannes Lohi, Ph.D.
Department of Basic Veterinary Sciences
Faculty of Veterinary Medicine
University of Helsinki
Helsinki, Finland

and

Professor Markku Pelto-Huikko, MD, Ph.D.
Department of Developmental Biology
Faculty of Medicine
University of Tampere
Tampere, Finland

Opponent

Professor Howard Jacobs, Ph.D.
Institute of Medical Technology
University of Tampere
Tampere, Finland

To my family

ABSTRACT

Anu Sironen

Molecular genetics of the immotile short tail sperm defect

The immotile short tail sperm (ISTS) defect is an autosomal recessive disease within the Finnish Yorkshire pig population. The defect is expressed in males as a shorter sperm tail length and immotile spermatozoa. Histological examination of spermatozoa from ISTS affected boars indicates that the axonemal complex and accessory structures of the sperm tail are severely compromised. Cilia in respiratory specimens from ISTS boars are physiologically normal and no adverse effects on reproductive performance of female relatives have been observed suggesting that other ciliated cell types are not influenced.

The principal aim of this study was to map the ISTS associated chromosomal region and develop a DNA-test for marker and gene assisted selection within the Finnish Yorkshire pig population. In the initial genome wide screen the disease locus was mapped on porcine chromosome 16 within a 3 cM region and a two-marker-haplotype was developed for marker-assisted selection within analyzed families. The disease associated region was further fine-mapped in order to develop a 100% specific test for carrier detection. The disease-associated area was located to a 2 cM region on human chromosome 5p13.2 and polymorphisms from orthologous porcine genes within this region defined the disease-associated haplotype to include 8 genes in the human. Sequence analysis of the most probable candidate, *KPL2,* revealed the presence of an inserted Line-1 retrotransposon within an intron. The insertion affects splicing of the *KPL2* transcript via skipping of the upstream exon or by causing the inclusion of an intronic sequence, as well as part of the insertion in the transcript. Both changes alter the reading frame leading to premature termination of translation. Since 2006 gene assisted selection for ISTS based on this insertion sequence has been made available to pig breeders in Finland.

KPL2 expression profiling revealed various tissue specific transcript variants. The long form of *KPL2* including the aberrantly spliced exon is expressed predominantly in porcine testicular tissue, which explains the tissue-specificity of the ISTS defect. Localization of the KPL2 protein in the murine testis and a possible interaction with IFT20 indicate a role in the delivery of flagellar proteins. Furthermore, the presence of KPL2 in the sperm tail midpiece also suggests a structural function in the sperm tail. Possible associations of the KPL2 protein with the Golgi complex and Sertoli cell/spermatid junction require further investigation.

Current results show that the *KPL2* gene is important for correct sperm flagella development. Disruption of this process is responsible for the ISTS defect in Finnish Yorkshire boars. Expression and interaction studies of the KPL2 protein allowed the function of KPL2 to be elucidated. Due to the highly conserved nature of spermatogenesis these results provide novel insights into sperm tail development and male infertility disorders in all mammalian species.

Keywords: sperm, flagella, ISTS, MAS, KPL2, Line-1

TIIVISTELMÄ

Anu Sironen

Hedelmättömyyttä aiheuttavan siittiöiden puolihäntävian molekyyligenetiikka

Suomalaisissa Yorkshire karjuissa yleistyi 1990-luvun lopulla autosomaalisesti ja resessiivisesti periytyvä hedelmättömyyttä aiheuttava siittiöiden puolihäntävika (ISTS, immotile short tail sperm). Sairaus aiheuttaa normaalia lyhyemmän ja täysin liikkumattoman siittiön hännän muodostuksen. Muita oireita sairailla karjuilla ei ole havaittu ja emakot ovat oireettomia. Tämän tutkimuksen tarkoituksena oli kartoittaa siittiöiden puolihäntävian aiheuttava geenivirhe ja kehittää DNA-testi markkeri- ja geeniavusteiseen valintaan.

Koko genomin kartoituksessa vian aiheuttava alue paikannettiin sian kromosomiin 16. Paikannuksen perusteella kahden geenimerkin haplotyyppi kehitettiin käytettäväksi markkeri-avusteisessa valinnassa. Sairauteen kytkeytyneen alueen hienokartoitusta jatkettiin geenitestin kehittämiseksi kantajadiagnostiikkaan. Vertailevalla kartoituksella oireeseen kytkeytynyt alue paikannettiin 2 cM:n alueelle ihmisen kromosomiin viisi (5p13.2). Tällä alueella sijaitsevia geenejä vastaavista sian sekvensseistä löydetyn muuntelun perusteella voitiin tarkentaa sairauteen kytkeytyneitä haplotyyppejä. Haplotyyppien perusteella puolihäntäoireeseen kytkeytynyt alue rajattiin kahdeksan geenin alueelle ihmisen geenikartalla. Alueelle paikannetun kandidaattigeenin (*KPL2*) sekvensointi paljasti introniin liittyneen liikkuvan DNA-sekvenssin, Line-1 retroposonin. Tämä retroposoni muuttaa geenin silmikointia siten, että sitä edeltävä eksoni jätetään pois tai myös osa introni- ja inserttisekvenssiä liitetään geenin mRNA tuotteeseen. Molemmissa tapauksissa tuloksena on lyhentynyt KPL2 proteiini. Tähän retroposoni-inserttiin perustuva geenitesti on ollut sianjalostajien käytössä vuodesta 2006.

KPL2 geenin ilmenemisen tarkastelu sialla ja hiirellä paljasti useita kudosspesifisiä mRNA muotoja. *KPL2* geenin pitkä muoto ilmenee pääasiassa vain kiveksessä, mikä selittää geenivirheen aiheuttamat erityisesti siittiön kehitykseen liittyvät oireet. KPL2 proteiinin ilmeneminen hiiren siittiön hännän kehityksen aikana ja mahdollinen yhteistoiminta IFT20 proteiinin kanssa viittaavat tehtävään proteiinien kuljetuksessa siittiön häntään. Mahdollisen kuljetustehtävän lisäksi KPL2 saattaa toimia myös siittiön hännän rakenneosana, koska se paikannettiin valmiin siittiön hännän keskiosaan. Lisäksi KPL2 proteiini saattaa myös toimia Golgin laitteessa sekä Sertolin solujen ja spermatidien liitoksissa, mutta nämä havainnot kuitenkin vaativat lisätutkimuksia.

Tämän tutkimuksen tulokset osoittavat, että *KPL2* geeni on tärkeä siittiön hännän kehitykselle ja sen rakennemuutos aiheuttaa siittiöiden puolihäntäoireen suomalaisilla Yorkshire karjuilla. KPL2 proteiinin ilmeneminen ja paikannus siittiön kehityksen aikana antaa viitteitä proteiinin toiminnasta. Koska *KPL2* geenisekvenssi on erittäin konservoitunut, nämä tulokset tuovat uutta tietoa kaikkien nisäkkäiden siittiöiden kehitykseen ja urosten hedelmättömyyden syihin.

Avainsanat: siittiö, siittiön häntä, ISTS, MAS, KPL2, Line-1

TABLE OF CONTENTS

ABBREVIATIONS

aa	amino acid
AK, ADK	adenylate kinase
AKAP	A-kinase anchoring protein
AMP	adenosine monophosphate
ASP	antisense promoter
ATP	adenosine-5'-triphosphate
BAC	bacterial artificial chromosome
BBS	Bardet-Biedl syndrome
BLAST	basic local alignment tool
cAMP	cyclic adenosine monophosphate
CB	chromatoid body
cDNA	complementary DNA
CDS	ciliary dyskinesia syndrome
CP	central pair
CPC	CP complex
CREM	cyclic AMP response element modulator
CS	central sheath
Dapi	4'6-diamidino-2-phenylindole
DFS	dysplasia of fibrous sheath
ECL	enhanced chemiluminescent
ES	elongating spermatids
EST	expressed sequence tag
FS	fibrous sheath
FSH	follicle stimulating hormone
FSH-R	FSH receptor
GAPDS	glyceraldehyde-3-phosphate dehydrogenase, spermatogenic
GAS	gene assisted selection
HPA	Helix pomatia agglutinin
ICS	immotile cilia syndrome
IDA	inner dynein arm
IFT	intra flagellar transport
IHC	immunohistochemistry
IMT	intramanchette transport
IP	immunoprecipitation
ISH	*in situ* hybridization
ISTS	immotile short tail sperm
Kbp	kilobasepair

kDa	kilodalton
LH	luteinizing hormone
LH-R	LH receptor
Line-1, L1	long interspersed nucleotide element 1
LNA	locked nucleic acid
MAS	marker assisted selection
miRNA	microRNA
mRNA	messenger RNA
MS	mitochondrial sheath
NCBI	national center for biotechnology information
ND	not definable
ODA	outer dynein arm
ODFs	outer dense fibres
OMDA	outer microtubule doublets of the axoneme
ORF	open reading frame
PFA	paraformaldehyde
PBS	phosphate buffered saline
PCD	primary ciliary dyskinesia
PCR	polymerase chain reaction
piRNA	Piwi-interacting RNA
PK-A	protein kinase-A
PKD	polycystic kidney disease
PND	postnatal day
PSc	pachytene spermatocyte
qPCR	quantitative real-time PCR
RS	round spermatid
RSH	radial spoke head
RSp	radial spoke
RT-PCR	reverse transcription PCR
SC	Sertoli cells
SDS-PAGE	sodium dodecyl sulphate polyacrylamide gel
SNP	single nucleotide polymorphism
SPATA	spermatogenesis associated
SPEF	sperm flagellar
TR	transverse ribs
UTR	untranslated region
WT	wild type

LIST OF ORIGINAL PUBLICATIONS

This study is based on the following original publications, which are subsequently referred to in the text by Roman numerals (I-IV) and selected unpublished data.

I   Sironen AI, Andersson M, Uimari P, Vilkki J. Mapping of an immotile short tail sperm defect in the Finnish Yorkshire on porcine Chromosome 16. Mamm Genome. 2002 Jan;13(1):45-9.

II   Sironen A, Thomsen B, Andersson M, Ahola V, Vilkki J. An intronic insertion in *KPL2* results in aberrant splicing and causes the immotile short-tail sperm defect in the pig. Proc Natl Acad Sci U S A. 2006 Mar 28;103(13):5006-11. Epub 2006 Mar 20.

III   Sironen A, Vilkki J, Bendixen C, Thomsen B. Infertile Finnish Yorkshire boars carry a full-length Line-1 retrotransposon within the *KPL2* gene. Mol Genet Genomics. 2007 Oct;278(4):385-91. Epub 2007 Jul 4.

IV   Sironen A, Hansen J, Thomsen B, Andersson M, Vilkki J, Toppari J, Kotaja N. Role of KPL2 in the organization of the sperm tail in differentiating mammalian germ cells. Submitted.

Original publications have been reproduced with the permission of copyright owners.

1. INTRODUCTION

Male infertility is a significant problem in humans and domestic animals (Lunenfeld B. 1993). In humans, it is estimated that 15% of couples are infertile and in one third of these cases infertility can be attributed solely to the male partner (Kolettis. 2003). In productive livestock the economic losses due to reproductive inefficiency in males can be substantial, particularly when infertility affects a genetically superior individual (Roberts J. 1986). Although some instances of male factor infertility can be explained by infections, environmental causes, immunological or hormonal deficiencies, many are caused by genetic factors. Problems with the production and maturation of spermatozoa are the most common causes of male infertility resulting in a low sperm count, morphologically abnormal spermatozoa or reduced sperm motility (Boyle et al. 1992, Linford et al. 1976, Wallace. 1992). The signaling pathways and molecular mechanisms that control the assembly and function of the normal mammalian sperm flagellum are not fully understood. The ultrastructure of mammalian spermatozoa is highly conserved and therefore knowledge of genes and proteins involved in sperm development in different animals can be used across species.

A reproductive problem in Finnish Yorkshire boars was detected in 1987, when the first boar with immotile short tail sperm (ISTS) defect was identified. The ISTS defect causes infertility due to short tailed and immotile spermatozoa and all affected sperm tail structures are typically severely compromised (Andersson et al. 2000). ISTS became common at the end of the 1990s. In year 2000, 37% of the Finnish Yorkshire population carried the defect representing a significant economic burden to Finnish pig breeding. Based on the segregation analysis of family material this defect was suggested to be inherited as an autosomal recessive disease, thus providing an opportunity to map a gene involved in sperm tail development. The ISTS disorder appears to be sperm specific, since no adverse effects on respiratory function or female reproduction have been identified (Andersson et al. 2000). Similar defects are known to occur in other species (Blom. 1976, Maqsood. 1951, Vierula et al. 1983) and identification of the disease causing mutation for ISTS may offer valuable insights into sperm development.

Due to the highly conserved structure of the axoneme within cilia and sperm flagella, resolving the molecular genetics of a sperm tail defect may provide insights into other ciliary defects. Cilia play important roles in many physiological processes, including cellular and fluid movement, sensory perception, signaling and development (Scholey and Anderson. 2006). Ciliary dysfunction has been implicated in several disorders and the number of cilia related defects is expected to increase (Fliegauf et al. 2007).

The ISTS defect in Finnish Yorkshire pig population provides an excellent opportunity to investigate the genetic background of a flagellar defect resulting in total infertility. Due to

the conserved nature of the axonemal structure and formation this study provides a novel insight into development of cilia/flagella and male infertility disorders in all mammalian species. Furthermore, this study provides tools for genetic testing against an infertility disorder within the Finnish Yorkshire pig population. Due to the genetic background of ISTS, a DNA-test is required to effectively reduce the impact and financial burden of the ISTS defect to Finnish pig breeding.

2. REVIEW OF THE LITERATURE

2.1 Spermatogenesis

Spermatogenesis occurs in the seminiferous tubules of the testis, where the spermatogenic stem cells are located near the basal lamina and surrounded by Sertoli cells (SC). Maturation of germ cells can be divided into three phases: 1) the proliferative phase (spermatogonia), in which spermatogonia undergo rapid divisions, 2) the meiotic phase (spermatocytes) in which genetic material is segregated and 3) differentiation (spermiogenesis, spermatids) in which spermatids transform into spermatozoa (Russel L.D., Ettlin R. A., Sinha H.A.P. and Legg E. D. 1990, Fig. 1). During the proliferative phase spermatogonia go through several mitotic divisions. The final mitotic division of differentiated spermatogonia gives rise to the primary spermatocytes. Meiosis of primary spermatocytes leads to the production of secondary spermatocytes after the first meiotic division, while haploid round spermatids are formed following the second meiotic division (Fig. 1). After meiosis, spermatids are connected with cytoplasmic bridges sharing transcripts and proteins (Ventela et al. 2003). In spermiogenesis the nucleus of germ cell is remodelled by chromatin condensation and the removal of excess cytoplasm, and the acrosome and sperm tail are formed. Finally, mature spermatozoa are released into the lumen of seminiferous epithelium and transported to the epididymis for further maturation.

Hormonal regulation is critical for germ cell development. The primary hormonal controls on spermatogenesis involve the action of follicle-stimulating hormone (FSH) and testosterone on SCs (Heckert and Griswold. 2002). FSH and luteinizing hormone (LH) are secreted by the anterior pituitary and act directly on the testis to stimulate somatic cell function in support of spermatogenesis (Holdcraft and Braun. 2004). The primary role of FSH in spermatogenesis is the stimulation of SC proliferation during development (Heckert and Griswold. 2002). FSH receptor (FSH-R) expression is limited to SCs (Rannikki et al. 1995), while LH receptors (LH-R) are found primarily in the Leydig cells (Lei et al. 2001). Testosterone has a primary role in germ cell development and is produced in Leydig cells under the hormonal regulation of LH (Mendis-Handagama. 1997).
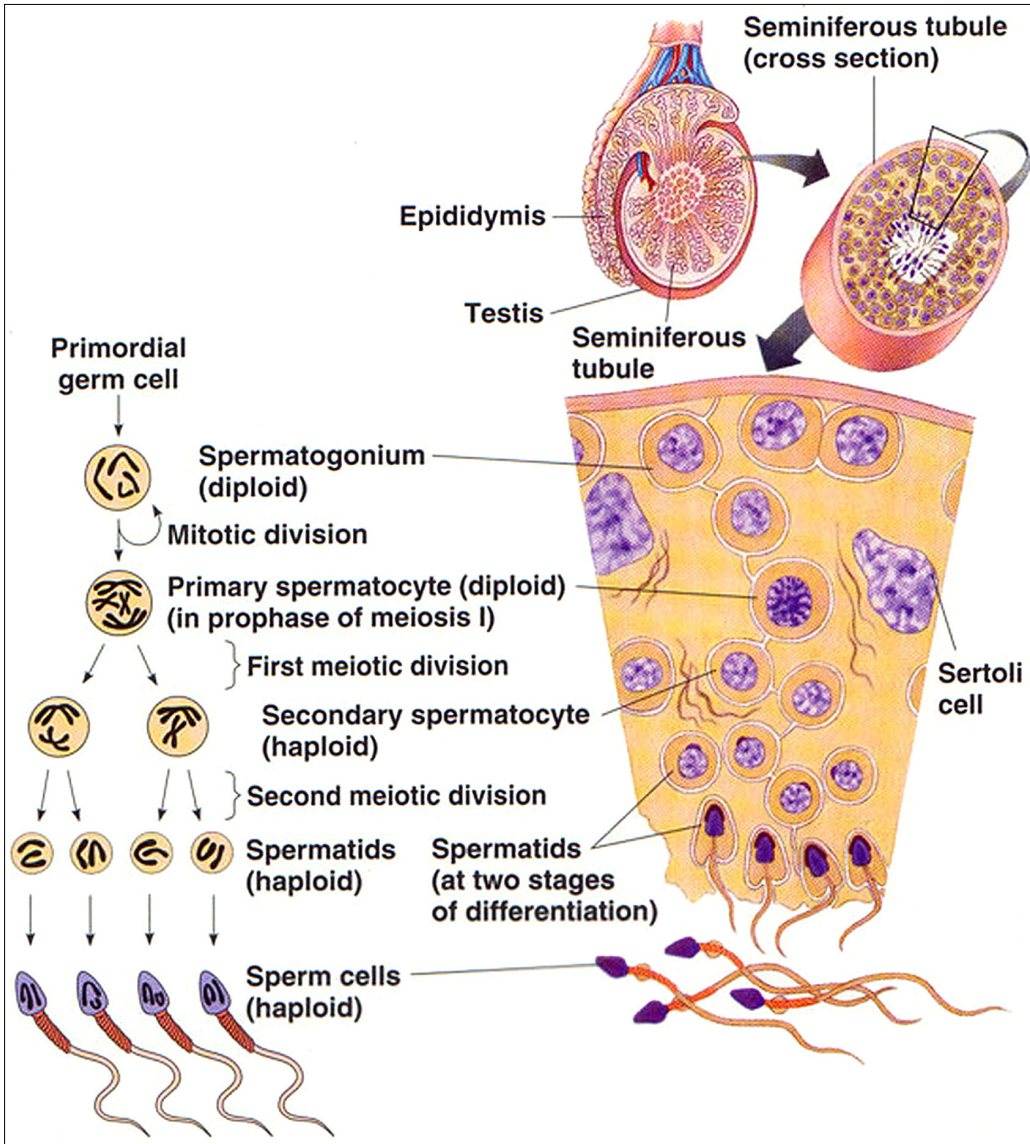
Figure 1. Schematic representation of spermatogenesis. Spermatogenesis starts with spermatogonia in the basal lamina continuing towards the lumen. Spermatogonia go through several mitotic divisions and finally form primary spermatocytes. The meiotic divisions give rise to haploid secondary spermatocytes and finally spermatids, which transform to spermatozoa during spermiogenesis. Figure available at http://faculty.sunydutchess.edu/scala/Bio102/default.htm.

Development of spermatogonia to haploid spermatids takes approximately 35 days in mice (Oakberg. 1957) and 64 days in humans (Heller and Clermont. 1963). The whole spermiogenetic period lasts about 2-3 weeks in mice and 5-6 weeks in humans (Tanaka and Baba. 2005). Seven-day-old mouse testes contain only SCs and spermatogonia in the seminiferous tubules. At nine days of age early spermatocytes appear, and at three weeks late spermatocytes are also present. Spermatids start to differentiate at postnatal

day (PND) 20 (Fig. 2) and sperm tail accessory structures appear around PND 30 in the mouse testis (Bellve et al. 1977). This germ cell differentiation is organized in seminiferous tubules. In the mouse, the seminiferous epithelium cycle can be divided into at least 12 stages (I–XII) with each stage containing a defined collection of cell types (Russel L.D., Ettlin R. A., Sinha H.A.P. and Legg E. D. 1990, Fig. 2).
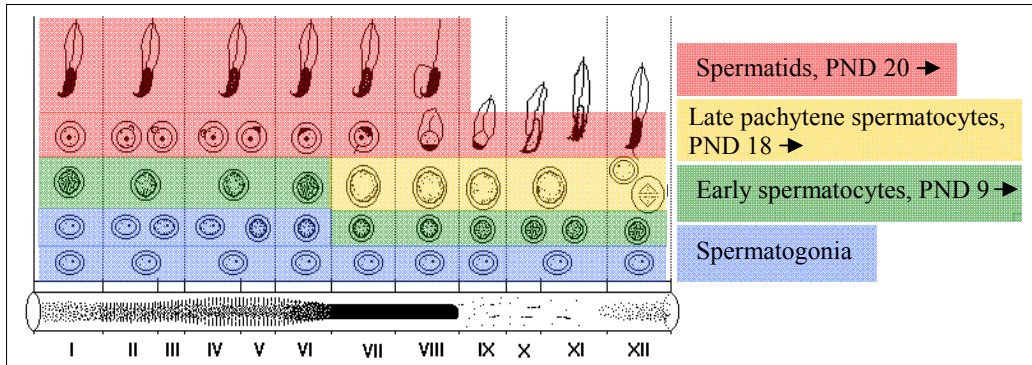
Figure 2. Schematic representation of the 12 stages (I–XII) in the mouse seminiferous epithelial cycle. Each stage is defined by a specific collection of cell types, which are classified by the morphology of the developing spermatids. During the first wave of spermatogenesis at PND 7 only Sertoli cells and spermatogonia are present in the seminiferous tubules. Early spermatocytes appear at PND 9 and at PND 18 pachytene spermatocytes are present. After meiotic divisions round spermatids start to differentiate at PND 20.

2.1.1 Functions of Sertoli cells

SCs are the only somatic cells in the seminiferous tubules and are essential for germ cell maturation. SCs have several important functions; provide physical support, form the testis-blood barrier, compartmentalize the seminiferous epithelium, provide nutrients and growth factors, take part in the translocation of germ cells, phagocytose apoptotic germ cells and secrete seminiferous tubular fluid (Griswold. 1998). SCs regulate germ cell movement by different junctions between SCs themselves and SCs and germ cells. Furthermore, SCs provide the developing germ cells with appropriate mitogens, differentiation factors and energy to protect them from harmful agents and the host's immune system (Petersen and Soder. 2006). Malfunction and deprived development of SCs during foetal life have been suggested to result in low sperm counts and testicular cancer (Petersen and Soder. 2006). Although many SC proteins have been identified, in the vast majority of cases the specific function with respect to germ cell development remains unknown.

2.1.1.1 Cell junction types in the testes

Accurate function of cell junctions is essential for sperm development. During spermatogenesis testicular cells interact through specialized junctions (Table 1). Tight

junctions create a blood-testis barrier between premeiotic and meiotic/postmeiotic germ cells (basal and adluminal compartment, respectively). It is a physical barrier between the blood vessels and the seminiferous tubules and prevents passage of macromolecules into the seminiferous tubules. Anchoring junctions maintain tissue integrity and may also function in signal transduction events. Modified types of anchoring junctions are ectoplasmic specializations, tubulobulbar complexes and focal contacts. Ectoplasmic specializations and tubulobulbar complexes are only found in the testis and both participate in spermiation. Moreover, ectoplasmic specializations are involved in translocation of spermatids during elongation. Tubulobulbar complexes are only visible a few days before spermiation and are believed to prevent the premature release of elongating spermatids. The exact roles of focal contacts and desmosomes in the testis have not yet been elucidated. In other tissues focal contacts operate in cell movement and in signal transduction, while desmosomes are important for tissue integrity. Hemidesmosomes connect the cellular cytoskeleton to the underlying basement membrane. Gap junctions mediate signals between SCs and germ cells playing a crucial role in germ cell movement in the seminiferous epithelium (Mruk and Cheng. 2004).

Table 1. Different cell junction types present in the testis and their function.

Junction type	Function in the testis (in other tissues)	Cells
Tight junctions	Form basal and adluminal compartment	SC
Anchoring junctions	Maintain tissue integrity	SC, SC-germ
Ectoplasmic specializations	Translocation of spermatids, spermiation, stabilization of other junctions	SC, SC-germ
Tubulobulbar complex	Spermiation	SC, SC-germ
Focal contact	May participate in cell adhesive function in ectoplasmic specialization (cell movement and in signal transduction)	Testicular cells and extracellular matrix
Desmosomes	Not known (tissue integrity)	SC, SC-germ
Hemidesmosomes	Connect the cell cytoskeleton to the underlying basement membrane	Testicular cells and extracellular matrix
Gap junctions	Signal transduction, germ cell movement	SC, SC-germ, Leydig cells

2.1.2 Gene expression in spermiogenesis

In order to complete the very complex development of spermatozoa, several specific transcriptional regulators are needed. Transcription is regulated via methylation and trans-acting factors that bind to the TATA-box, the CRE-box, or other specific DNA sequences in the promoter region (Steger. 1999). An important regulator of spermatid specific transcription is the cyclic AMP response element modulator (CREM, Hogeveen and Sassone-Corsi. 2006). In CREM-knockout mice, males are infertile and spermatogenesis is arrested at the round spermatid phase (Blendy et al. 1996, Nantel et al. 1996). However, some spermatid specific proteins do not contain CRE-motifs in their promoter regions suggesting that other regulatory mechanisms may also exist (Tanaka and Baba. 2005).

Most of the transcription during spermiogenesis occurs in round spermatids, since transcription and translation are repressed during spermiogenetic differentiation. However, transcription of specific genes can take place during the very late phases of spermiogenesis. Transcripts are stored as ribonucleoprotein particles in a translationally repressed state and are translated in elongating spermatids (Tanaka and Baba. 2005). After meiosis the intercellular bridge enables the transport of mRNA between haploid spermatids (Russel L.D., Ettlin R. A., Sinha H.A.P. and Legg E. D. 1990). The chromatoid body (CB) is a structure that has been suggested to collect mRNAs and function as a subcellular co-ordinator of different RNA-processing pathways in spermatids (Kotaja et al. 2006,Kotaja and Sassone-Corsi. 2007). Post-transcriptional mRNA regulation by microRNA (miRNA) and RNA interference pathways play a role in spermatogenesis, as well as in somatic cells. The block of miRNA production by testis specific knock-out of dicer, which is a crucial enzyme in miRNA processing, causes subfertility (Maatouk et al. 2008). Recent research has revealed the importance of testis specific small noncoding RNAs (Piwi-interacting RNAs, piRNAs) in spermatogenesis. Deletion of the genes encoding piwi family members in the mouse leads to the block of spermatogenesis at spermatocyte or round spermatid stages (Kuramochi-Miyagawa et al. 2004, Deng and Lin. 2002). It is not clear if piRNAs primarily control chromatin organization, gene transcription, RNA stability or RNA translation (Klattenhoff and Theurkauf. 2008). However, piRNAs are known to be involved in retrotransposon silencing (Aravin et al. 2007).

2.2   Epididymal sperm maturation

After development in the testis spermatozoa are immotile and unable to penetrate into the oocyte. The ability to fertilize is achieved during sperm maturation in the epididymis. Furthermore, spermatozoa are stored and protected by the epididymis. The epididymis is divided into three parts; caput, corpus and cauda. Most spermatozoa attain their full fertilizing capacity in the proximal cauda. While the caput and corpus epididymis are responsible for sperm maturation, the cauda epididymis is involved in sperm storage ensuring that male gametes are available in sufficient numbers at ejaculation (Sullivan. 2004).

The cellular processes responsible for sperm maturation are triggered by changes in the cell membrane of spermatozoa. Most of the testicular proteins entering the epididymis are rapidly reabsorbed in the caput. During epididymal passage of sperm, the epididymal epithelium secretes proteins that interact with the transiting spermatozoa. Most of the proteins are secreted in the caput, but the content varies from one segment to another modifying the maturing spermatozoa. Several surface proteins of spermatozoa disappear or are processed during epididymal transit, but several new proteins also appear (Dacheux et al. 2003).

2.3   Structure of the mammalian sperm tail

During spermiogenesis the correct assembly of the sperm tail is required for functional spermatozoa. Mammalian sperm tail consists of the axoneme and accessory structures; the mitochondrial sheath (MS), outer dense fibres (ODFs) and the fibrous sheath (FS). The axoneme is highly conserved in all ciliated and flagellated eukaryotic cells, but only mammalian sperm flagella contain the accessory structures. These accessory structures are known to be critical for motility of the sperm tail and abnormalities in these structures result in severe malformations in sperm flagella. A connecting piece attaches the sperm head to the flagellum, which consists of three distinct regions: the midpiece, the principal piece and the end piece. Common to these three segments is the axoneme that runs the entire length of the flagella (Cao et al. 2006a). The midpiece is proximal to the sperm head and contains the mitochondrial sheath including all the mitochondria of sperm, which are helically arranged around the ODFs. The midpiece is separated from the principal piece by a septin-based ring-like structure; the annulus (Ihara et al. 2005, Kissel et al. 2005, Steels et al. 2007). Seven of the nine ODFs extend through the principal piece, while fibres 3 and 8 are replaced by the longitudinal columns of the FS that are connected by numerous regularly spaced circumferential ribs (Fig. 3). The FS underlies the cell membrane and encases the ODFs and axoneme. The end piece consists of the axoneme surrounded by the cell membrane (Cao et al. 2006a).

The role of ODFs is to provide passive elasticity to the flagellum. Several ODF proteins have been characterized, but there are no reports on targeted mutations affecting any of the ODF specific genes (Turner. 2003). The major ODF protein is ODF1 (Burmester and Hoyer-Fender. 1996, Hoyer-Fender et al. 1995), which interacts with several other proteins localized to ODFs [ODF2, SPAG4, SPAG5, OIP1 (Shao et al. 1999, Shao et al. 2001, Zarsky et al. 2003)]. Another cytoskeletal structure of the sperm flagella is the FS. Traditionally it has been thought that this structure provides rigid support for the flagellum (Fawcett. 1975), but more recent evidence suggests a further active role in sperm motility. A growing number of regulatory proteins involved in pathways regulating motility and metabolism have been localised to FS including several glycolytic enzymes (Turner. 2003). Two major structural proteins of FS are A-kinase anchoring proteins 3 and 4 (AKAP3, AKAP4). AKAP3 is reported to be involved in organizing the basic structure of the FS, whereas AKAP4 has a major role in completing the FS assembly (Baccetti et al. 2005b). The absence of AKAP4 diminishes sperm motility resulting in infertility (Eddy et al. 2003). Another FS associated protein spermatogenic glyceraldehyde-3-phosphate dehydrogenase (GAPDS) has also been shown to reduce motility in the GAPDS-null mouse model (Miki et al. 2004) supporting the hypothesis that FS has more diverse functions than simply supporting the flagella (Brown et al. 2003). Furthermore, some identified FS proteins indicate that the FS protects sperm from oxidative stress (Eddy et al. 2003). Although genomic and proteomic studies have

increased our knowledge of sperm tail components, the exact functions and interactions of these proteins are largely unknown.
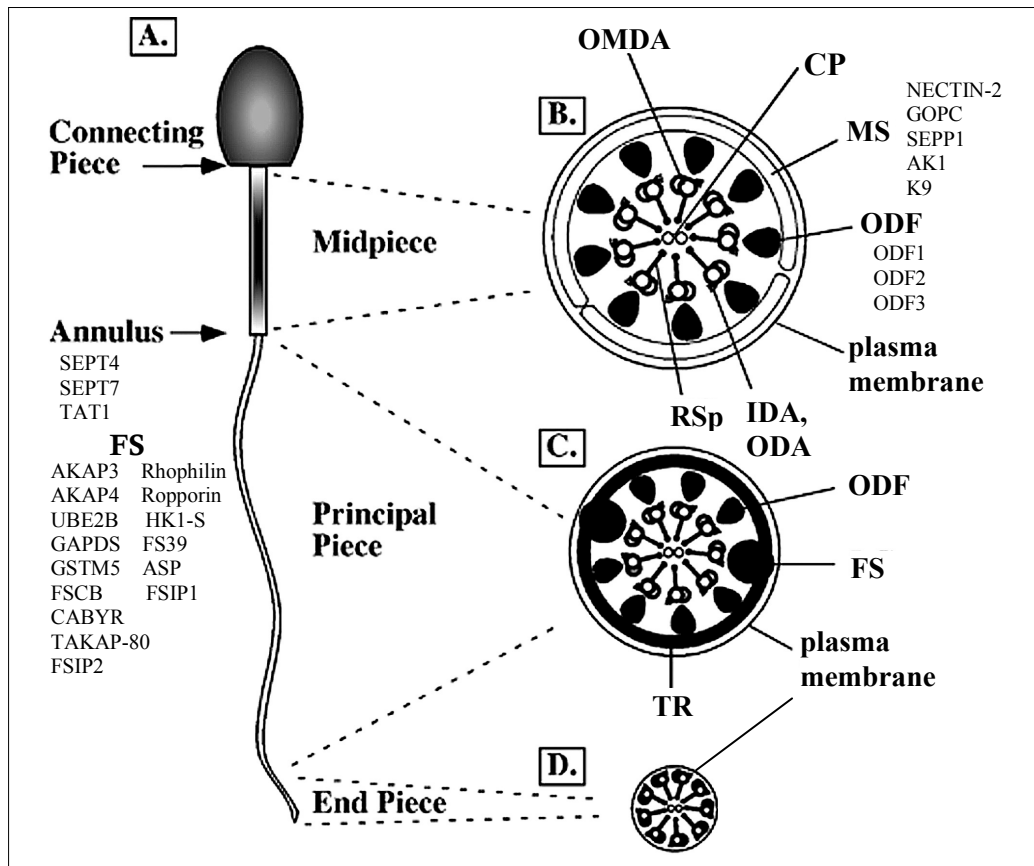

Figure 3. Schematic representation of mammalian sperm as seen in longitudinal section (left side) and in cross-sections (right side). **A.** The mammalian sperm flagellum is anchored to the nucleus by the connecting piece and consists of three segments: the mid piece, the principal piece and the end piece. The distal part of the mid piece and the proximal part of the principal piece are separated by the annulus. **B.** Schematic cross-section of the mid piece showing the plasma membrane and mitochondrial sheath (MS) surrounding the nine outer dense fibres (ODFs). Within the ODFs are the components of the axoneme: nine outer microtubule doublets of the axoneme (OMDA) with associated dynein arms (IDA and ODA), radial spokes (RSp) and the central pair of microtubule doublets (CP). **C.** Schematic cross-section of the principal piece showing the plasma membrane surrounding seven ODFs. Two ODFs are replaced by the longitudinal columns of the fibrous sheath (FS). The two columns are connected by transverse ribs (TR). The axonemal components are unchanged. **D.** Schematic cross-section through a representative segment of the end piece. The ODFs and FS taper at the termination of the principal piece and are no longer present in the end piece, thus leaving only the plasma membrane to surround the axoneme. The proteins found to be involved in the assembly and maintenance of the specific peri-axonemal structures of the mouse sperm flagellum are listed (Ihara et al. 2005, Baccetti et al. 2005b, Eddy et al. 2003, Miki et al. 2004, Escalier. 2006, Cao et al. 2006b, Shao et al. 1997, Brohmann et al. 1997, Petersen et al. 2002, Naaby-Hansen et al. 2002, Catalano et al. 2001, Li et al. 2007). Furthermore, several proteins have been shown to be involved in the assembly of various accessory structures. Figure modified from Turner. 2003, copyright by The American Society of Andrology.

2.3.1 Sperm tail formation

Formation of the sperm tail is a complex process starting in early spermatids. One of the two centrioles forms an axoneme and rapidly extends into the tubular lumen. After extension, the axoneme is implanted into the nucleus opposite to the acrosome. Thereafter, the accessory components are added to the flagellum to form the middle, principal and end pieces. During midspermiogenesis ODFs develop in close association with the nine outer doublets of the axoneme (Fawcett and Phillips. 1969). They originate as thin filaments from the proximal end of the midpiece and after elongation increase in thickness (Irons and Clermont. 1982, Oko and Clermont. 1989, Clermont et al. 1990). The formation of FS occurs throughout most of spermiogenesis. The FS is assembled from the distal end of the principal piece (Turner. 2003) and after elongation becomes connected by circumferential TR. The assembly of FS also supports the presence of the intra flagellar transport (IFT) machinery in the sperm flagella. The midpiece develops when the annulus migrates distally to the proximal end of the FS. Mitochondria assemble in a helical arrangement around the ODFs behind the migrating annulus (Turner. 2003). The motility of the sperm is achieved in the epididymis and in the female reproductive tract (Russel L.D., Ettlin R. A., Sinha H.A.P. and Legg E. D. 1990).

2.3.2 Flagella motility

The fertilizing capacity of spermatozoa requires sperm motility. Motility of flagella is based on the axoneme containing inner and outer dynein arms attached to outer doublet microtubules. Dynein arms provide the ATP dependent force for the movement of cilia and flagella by sliding of adjacent outer doublet microtubules and the central pair and radial spoke (CP/RSp) structures regulate dynein arm activity (Omoto et al. 1999, Porter and Sale. 2000).

2.3.2.1 Energy synthesis for flagellar motility

Proper sperm function depends on an adequate and continual supply of ATP, which induces the dyneins to bind to the B tubule (the incomplete pair of the doublet microtubule, Fig. 4) resulting in sliding between pairs of outer doublets (Silflow and Lefebvre. 2001). The motile wave of spermatozoa is propagated along the length of the flagellum, highlighting a requirement for ATP throughout the tail (Cao et al. 2006a). In the mammalian flagellum, ATP is generated in two distinct regions of the sperm tail; by oxidative phosphorylation in mitochondria localized to the midpiece and by glycolytic enzymes in the FS of the principal piece (Cao et al. 2006a, Miki. 2007). Although the functions of flagellar mitochondria are very similar to that in somatic cells, several unique proteins or protein isoforms have been found in the mitochondria of sperm tails (Burgos et al. 1995, Travis et al. 1998). Similar to the proteins of flagellar mitochondria, the glycolytic enzymes in the principal piece are distinct from the isozymes in somatic

cells (Miki et al. 2004, Boer et al. 1987, Welch et al. 2000, Feiden et al. 2008). An absence of one of the germ cell-specific isozymes, GAPDS, blocks glycolysis resulting in infertility of male mice (Miki et al. 2004). The results from GAPDS knockout mice indicate that most of the energy required for sperm motility is generated by glycolysis. Furthermore, mice lacking the testis-specific cytochrome c_T are fertile (Narisawa et al. 2002) indicating that glycolysis, but not oxidative phosphorylation, is essential for sperm motility and fertility. Even though oxidative respiration is not necessary for fertility, mutations affecting the mitochondrial activity do affect sperm motility and reduce the level of ATP (Narisawa et al. 2002, Ruiz-Pesini et al. 2007). Furthermore, defects in mitochondrial sheath formation are also often present in infertile male knockout mice such as Gopc -/- and Nectin-2 -/- (Bouchard et al. 2000, Suzuki-Toyota et al. 2004).

In addition to oxidative phosphorylation and glycolysis, ATP can be produced via adenylate kinase (AK). AK1 and AK2 have been identified in the accessory structures of the sperm tail. AK2 is present in the MS and AK1 in the ODF/microtubular doublet interface (Cao et al. 2006b). Furthermore, other AK isoforms have been detected in the testis, but their function remains unclear. Similar to mammalian sperm, no ATP transport shuttle system has been detected in *Chlamydomonas reinhardtii*. A *Chlamydomonas* AK is anchored by two outer dynein arm proteins, ODF5p and Oda10p (Wirschell et al. 2004). Another *Chlamydomonas* protein, CPC1, is found in the central pair of the axoneme and contains an unusual AK domain (Zhang and Mitchell. 2004). Homologues of CPC1 have been found in mammalian species, suggesting that additional proteins with AK properties are present in the axoneme. The presence of two proteins with AK activity explains why mutations of either protein alone reduce, but do not totally eliminate motility in *Chlamydomonas*.

2.3.2.2 Control of dynein arm activity

The generation of a normal flagellar waveform requires that the activation and inactivation of the dynein arms occur in an asynchronous manner, which is achieved by interactions of CP/(RSp in *Chlamydomonas* (Wargo and Smith. 2003). Phosphorylation of the axonemal dynein by cAMP/PK-A pathway activates the dynein ATPase and dephosphorylation by calcium reverses activation (Turner. 2003, Turner. 2006). Mutagenesis studies in *Chlamydomonas* have revealed several genes (e.g. *pf18, pf19, pf20, pf6, pf16,* and *pf15*) coding for the central apparatus proteins, dysfunction of which cause the paralysis of flagella (Adams et al. 1981,Horowitz et al. 2005) highlighting the function of CP/RSp structures in controlling dynein arm activity (Omoto et al. 1999, Porter and Sale. 2000, Smith and Lefebvre. 1997). The importance of the central pair and radial spoke (CP/RSp) structure for motility suggests a function of this structure in signaling pathways of the activation/ inactivation of dynein arms. High levels of ATP are thought to inhibit the outer arms by binding to a regulatory site on an outer arm dynein heavy chain (Omoto et al. 1996), which

is overridden by the CP/RSp complex resulting in the activation of the inner arms in a co-ordinated fashion (Porter and Sale. 2000). Evidence from an additional control system that inhibits dynein activity suggests a group of suppressors (*sup-pf-1*, *sup-pf-2, pf2*, *pf3*, *pf9-2*, *sup-pf-3*, *sup-pf-4*, and *sup-pf-5,* Porter and Sale. 2000), which may involve changes in the regulatory sites that otherwise inhibit dynein activity at physiological levels of ATP (Rupp et al. 1996). Mutations in *pf16* (*Spag6*) and *pf20* (*Spag16*) have also been shown to affect spermatogenesis in the mouse, where SPAG6 interacts with SPAG16. Moreover, mutated *Spag6* and *Spag16* are known to cause infertility and truncated flagella (Escalier. 2006, Zhang et al. 2004, Sapiro et al. 2002).

2.4   Cilia and flagella

The highly conserved structure of the axoneme of cilia and flagella indicates the involvement of similar structural components and developmental processes in both organelles. Cilia and flagella are both thin, microtubule-based projections surrounded by specialized ciliary membrane. Although all cilia and flagella have a very similar internal arrangement of the cytoskeletal structure, they exhibit a distinctive pattern of movement (Pan et al. 2005). Furthermore, flagella are longer in length than cilia and cells may only contain one or two flagella, whereas multiple cilia may be present.

Cilia are present in the majority of mammalian cells and play important roles in many physiological processes, including cellular and fluid movement, sensory perception, signaling and development (Scholey and Anderson. 2006). For example, in the skin, cilia are essential for hair development probably through reception of signals from the sonic hedgehog signaling pathway (Lehman et al. 2008). In the eye, the rod and cone photoreceptors function in vision depends on the formation of a sensory cilium (Insinna and Besharse. 2008). The role of cilia in these sensory neurons is well established and intensive research on the role of cilia over the past decade has revealed that cilia are important sensory antenna in many tissues. In the kidney, cilia also function as a flow sensor facilitating increases in intracellular calcium concentration when required (Deane and Ricardo. 2007). Motile cilia are important for mucus clearance from the trachea and lungs as well as for transport of ovum in the female reproductive tract. A similar mechanism of axonemal movement is necessary for sperm motility and male fertility.

The internal cytoskeletal structure of cilia, flagella, basal bodies and centrioles is the highly conserved axoneme (Inaba. 2003, Hackstein et al. 2000). The axoneme structure consists of nine outer doublet microtubules either surrounding a central pair of singlet microtubules (9+2 cilia) or without central microtubules (9+0 cilia). In motile cilia, the outer doublet microtubules contain motor complexes, the inner and outer dynein arms (IDA and ODA, respectively), which are different in function and composition (Porter

and Sale. 2000, King. 2000). Mutations in genes encoding IDA components result in changes in the waveform, whilst mutations affecting ODA reduce beat frequency (Silflow and Lefebvre. 2001). Neighbouring peripheral doublet microtubules are linked to each other by the elastic protein nexin and are also connected to the inner singlets by RSp (Fig. 4).
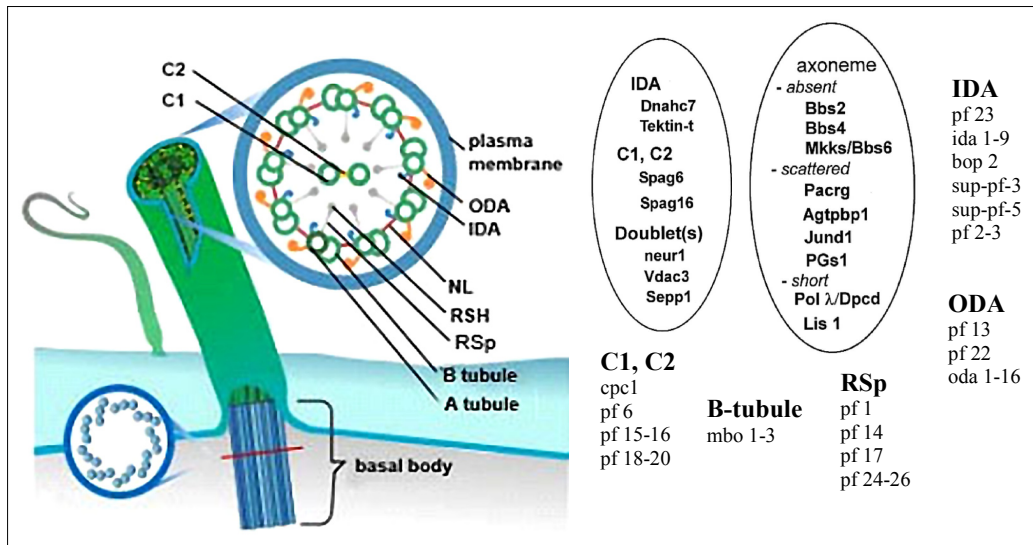

Figure 4. Schematic of cilia structure and cross section of 9+2 axoneme. The basal body templates the assembly of the axoneme within cilia membrane. The outer and inner dynein arms (ODA and IDA, respectively) are attached to the nine microtubule doublets (A and B tubule) and are made up of multiprotein complexes. The doublets are connected to each other by nexin links (NL). The axonemal central apparatus consists of the C1 and C2 microtubules, bridges between C1 and C2 and the central sheath. The RSps extend from each doublet, the radial spoke heads (RSH) being adjacent to the central sheath. The *Chlamydomonas* mutants that affect the assembly or function of specific structures are listed [list modified from (Porter and Sale. 2000, Yagi et al. 2005, Pazour and Witman. 2000, Ahmed and Mitchell. 2005)] and the proteins found to be involved in the assembly and maintenance of the mouse sperm flagellar axoneme are circled (Escalier. 2006).

In addition to motile cilia, almost every cell in vertebrates contains a single primary cilium. Many of the primary cilia are missing central pair and the dynein arms, and some outer microtubules may be singular or contain fewer than nine doublets (Pan et al. 2005). Even though the primary cilia are mainly non-motile, the IFT machinery is involved with moving rafts loaded with cargoes, such as signal enzymes, receptors and ion channel components, from the centriolar basal body up to the tip of the cilium. When the transported cargo is released at the tip of the cilium, the transporters are reloaded with spent components or products of the membrane signal devices that are carried down to the basal body for disposal (Whitfield. 2004, Fig. 5). The IFT machinery is not only necessary for transport, but is also important for the sensory

activity of cilia through cilia-specific receptors, ion channels and signaling molecules (Fliegauf et al. 2007).

The structural proteins of cilia and flagella are highly conserved across species and much of the knowledge on their structure and function comes from studies of the unicellular, biflagellated green alga, *Chlamydomonas reinhardtii.* More than 200 proteins have been identified in the axoneme and at least an equal number of proteins are involved in assembly of the flagella (Silflow and Lefebvre. 2001). More than 25 mutations affecting the assembly of the axoneme and 52 mutations affecting the motility have been identified (Turner. 2003, Porter and Sale. 2000, Fig. 4). The discovery of axonemal genes in *Chlamydomonas* has contributed to the identification of genes involved in mammalian axoneme assembly. More recently knockout mouse models have increased our understanding of genetic factors necessary for mammalian sperm tail development (Escalier. 2006, Fig. 4). However, the molecular mechanisms behind the development of axonemal and periaxonemal structures remain poorly understood.

2.4.1 Assembly of cilia and flagella

The basal body templates the assembly of the axoneme (Pan et al. 2005, Fig. 4) which projects directly from one centriole. All components of cilia are synthesized in the cell body and transported into cilium by IFT. The IFT system comprises large protein complexes called IFT-particles and at least two motor proteins. The particles are transported from the basal body to the tip of the cilium by kinesin-2 motors (anterograde IFT) and in the reverse direction by IFT-dynein (retrograde IFT, Fig. 5). As first discovered in *Chlamydomonas,* this IFT system is conserved in all eukaryotes with only a few exceptions (Pan et al. 2005). In addition, the intramanchette transport (IMT) has been indicated to be central for the sperm tail assembly besides being crucial to the shaping and condensation of the sperm nucleus (Kierszenbaum. 2002). The manchette is a male germ cell-specific microtubular platform that functions during spermiogenesis as a storage and sorting centre for structural and signalling proteins (Fig. 5). Several findings suggest that the manchette may sort structural proteins to the centrosome and developing sperm tail (Kierszenbaum. 2001, Rivkin et al. 1997, Tres and Kierszenbaum. 1996). The regulation of flagellar assembly/disassembly is not yet well understood, but recent studies in *Chlamydomonas* indicate that homologues of signalling proteins and proteins involved in the control of the mitotic spindle apparatus play a key role in controlling flagellar length (Pan et al. 2005).
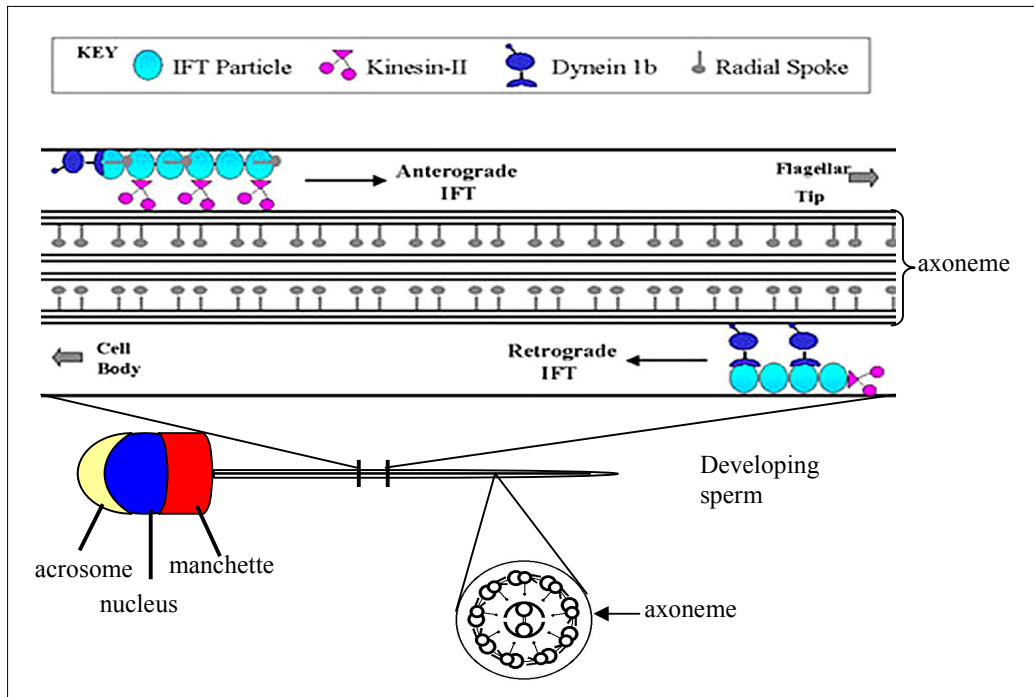
Figure 5. Intraflagellar transport is required for cilia/flagella formation, maintenance and sensory activity. Kinesin motor proteins transport IFT-particles with their cargo to the tip of the cilia and after reloading IFT-particles are carried down to the basal body by dynein motor proteins (modified from http://www.yale.edu/rosenbaum/rosen_research.html).

2.5 Cilia-related disorders

Cilia dysfunction has been implicated in several disorders and the number of these cilia related defects is expected to increase (Fliegauf et al. 2007). Cilia have been shown to be present in most cell types and therefore mutations in cilia related genes can lead to disorders in multiple tissues. Mutations in proteins that function in basal bodies, IFT machinery, axonemes, ciliary matrix and ciliary membrane can lead to cilia related diseases such as polycystic kidney disease (PKD), retinal dystrophy, neurosensory impairment, Bardet-Biedl syndrome (BBS) or primary ciliary dyskinesia (PCD, Ansley et al. 2003, Katsanis et al. 2001, Pazour and Rosenbaum. 2002, Van's Gravesande and Omran. 2005). Recent studies have documented the sensory roles of cilia for normal function of many tissues and raised the possibility that cilia are involved in energy metabolism and the regulation of blood pressure (Pan et al. 2005, Satir and Christensen. 2008). Furthermore, recent research indicates that cilia assembly and disassembly are closely related to cell-cycle control, and therefore may be associated with mechanisms involved in oncogenesis (Fliegauf et al. 2007).

2.5.1 Primary ciliary dyskinesia

As one of the first cilia related disorders, Kartagener in 1933 described a unique syndrome characterized by sinusitis, situs inversus and bronchitis (Kartagener syndrome, Lupin and Misko. 1978). Later, Afzelius made the connection between the syndrome and cilia introducing the term immotile cilia syndrome (ICS, Afzelius. 1976). Further studies showed that the disorganized motion of cilia resulted in ciliary defects leading to the term ciliary dyskinesia syndrome (CDS). At present, the term primary ciliary dyskinesia is used to describe the genetic defect, since transient ciliary dyskinesia may also be caused by environmental factors.

PCD is a genetically heterogeneous group of disorders with cilia dysfunction usually inherited as an autosomal recessive disease (Zariwala et al. 2007). PCD is characterized by altered motility or even the absence of cilia caused by defects in cilia structural/ motor components. Most common symptoms are defective mucociliary clearance, randomization of left-right body asymmetry and male infertility. Some PCD patients also exhibit heart disease, female subfertility, hydrocephalus, anosmia, retinitis pigmentosa and PKD (Pan et al. 2005). Structural defects have been observed in several axoneme components including ODA and IDA, RSp, nexin links and microtubules. Thus far, only mutations in genes *DNAI1, DNAI2, DNAH5, DNAH11, TXNDC3* and *KTU* encoding for proteins of dynein arms have been identified (Pennarun et al. 1999, Loges et al. 2008, Olbrich et al. 2002, Bartoloni et al. 2002, Omran et al. 2008, Duriez et al. 2007). In rare cases, X-linked inheritance of PCD has also been connected to the genes RPGR (Moore et al. 2006) and OFD1 (Budny et al. 2006). The fact that any one of the several defects in the motor mechanism of cilia can lead to dysfunction or total immotility may explain the relatively high frequency of ICS and also account for the failure to establish a linkage. The clinical features of patients suffering from PCD also vary significantly (Chodhari et al. 2004). Males with immotile spermatozoa usually have defective cilia in other ciliated tissues. However, cases have been reported where patients have immotile sperm, yet the structure and motility of other examined cilia are normal, or in patients with no history of respiratory tract disorders (Afzelius. 2004, Okada et al. 1999, Neugebauer et al. 1990).

2.5.1.1 Dysplasia of the fibrous sheath

A new variant of ICS was found in 1990, when dysplasia of the fibrous sheath (DFS) was detected (Chemes et al. 1990). The familial incidence of DFS suggests that the defect is of genetic origin (Chemes et al. 1998, Baccetti et al. 1993, Baccetti et al. 2001), although genetic and environmental interactions have been postulated (Chemes. 2000). DFS is one of the most severe abnormalities of sperm flagellar structure causing major alterations in the FS and affects various cytoskeletal components such as microtubules and ODFs leading to immotility (Chemes et al. 1998). Another structure frequently distorted in DFS spermatozoa is the mitochondrial sheath, which is caused by failure in the migration

of the annulus. Furthermore, in some cases the 9+2 axonemal structure is completely distorted (Rawe et al. 2001). Complete and incomplete forms of DFS have been described, where all, or between 70 and 80% of sperm tails are affected, respectively (Chemes et al. 1998). The testicular origin of the defect has been confirmed by the presence of similar alterations in immature spermatids (Rawe et al. 2001, Barthelemy et al. 1990).

To date, little is known about the genetic causes of DFS. It has been associated with pericentric inversion of human chromosome 9 (Baccetti et al. 1997) and with different Y microdeletions (Baccetti et al. 2005b). In mice, targeted disruption of the *Akap4* gene caused defects in sperm flagellum and motility. *Akap4* was only transcribed in the postmeiotic phase of spermatogenesis, and the fibrous sheath components were present, but the final structure was not complete and the flagellum was short (Miki et al. 2004). A possible relationship between deletions in *AKAP3* and *AKAP4* has also been suggested in one patient with DFS (Baccetti et al. 2005a). Thus far, no gene mutations causing DFS have been reported.

2.5.1.1.1 Immotile short tail sperm defect

The "stump" and "short tail" sperm defects have been described in several mammalian species (Andersson et al. 2000, Blom. 1976, Maqsood. 1951, Vierula et al. 1983) and belong to the DFS phenotype. These tail anomalies are characterized by short or irregular flagella with disorganized axonemes and a redundant FS (Baccetti et al. 2005b). In the Finnish Yorkshire (Large White) pig population a novel immotile short tail sperm (ISTS) defect has been identified as an autosomal recessive disease. The ISTS defect is exclusively expressed in male individuals resulting in total infertility. The first case in pigs was detected in Finnish Yorkshire boars in 1987 (Andersson et al. 2000). Nine new cases were identified in 1998. By 2001, the frequency of the mutation was as high as 23%.

Boars having the ISTS syndrome express the short tail characteristic sometimes with rudimentary or coiled tails and have lower sperm counts that classify the defect as DFS. Approximately 5% of spermatozoa from affected boars have tails of normal length, but none are motile. Sperm heads appear to develop normally, but cytoplasmic droplets were abundant (Sukura et al. 2002, Fig. 6). Histological examination of spermatozoa from affected boars indicates that the axonemal complex is severely compromised (Andersson et al. 2000). In most sections, one or both central microtubuli are absent, and in many cross-sections less than nine doublets are present. In addition, the ODFs and mitochondrial sheath are often disorganized and the midpiece and the principal piece of the sperm tail are reduced in length (Fig. 6). ISTS is manifested during spermiogenesis and it appears to affect spermatogenesis at the spermatid elongation phase, since only the number of elongated spermatozoa is reduced in affected boars (Sukura et al. 2002). Furthermore, conspicuous lipid droplets are present in the basal cytoplasm of SCs,

which is often caused by incomplete degradation of immature germ cells. It has been speculated that the defect may also be due to abnormal SC function (Sukura et al. 2002). No adverse effects on reproductive performance of female relatives have been observed, suggesting that structures, such as oviduct cilia, are not affected. Furthermore, cilia in respiratory specimens and in ductuli efferentes from affected boars are physiologically normal (Andersson et al. 2000). Therefore, the defect appears to be sperm tail specific and may be caused by a gene mutation that affects sperm tail development in particular.
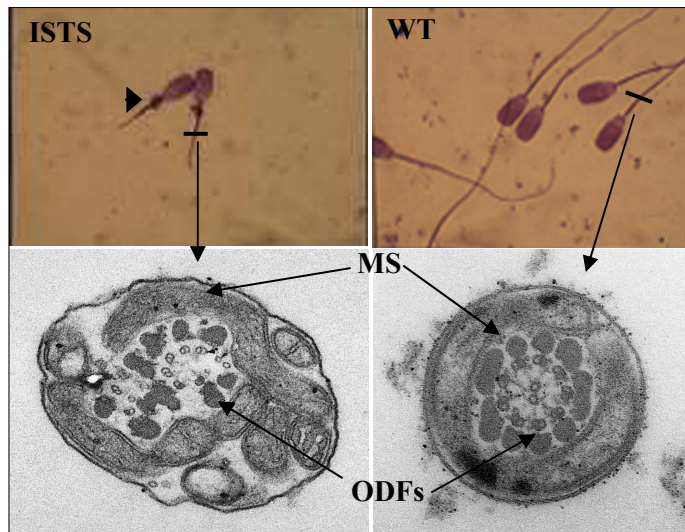

Figure 6. Structure of sperm of ISTS and normal (WT) boars. Sperm tail of ISTS affected boars is short and the proximal droplet (arrowhead) is retained in the neck region. The axoneme and accessory structures (MS, ODFs, indicated by arrows) of the ISTS flagella are also disorganized.

3. AIMS OF THE STUDY

The ISTS defect became a significant reproductive problem within the Finnish Yorkshire pig population at the end of 1990s and appeared to be a genetic disorder. Therefore, a genetic tool for marker- and gene-assisted selection was needed in order to decrease the severity and economic impact of this defect. Since sperm development is highly conserved among mammalian species, this defect in pigs also serves as a good model for understanding spermatogenesis and male infertility in humans. The main aims of the current study were:

1. To map the ISTS locus at chromosomal level and fine map the associated region within the Finnish Yorkshire pig population

2. To identify and characterize the mutation causing the ISTS defect in Finnish Yorkshire boars

3. To develop a DNA-test for the ISTS defect

4. To elucidate the role of the affected gene and protein during sperm tail development

4.   MATERIALS AND METHODS

Details of the laboratory methods can be found in the original publications (I-IV).

4.1   Animal material (I-IV)

For genotyping studies, samples of sperm or blood from 65 ISTS affected boars, 41 unaffected family members and 11 control boars were collected in boar stations or by a local veterinarian. Murine and porcine tissue samples for RNA or protein extraction were collected immediately after sacrifice, frozen in liquid nitrogen or preserved in RNAlater buffer (Qiagen) and stored at -80ºC. C57BL/6 mice were provided by The Central Animal Laboratory services in Turku. Pig tissue samples for RNA and protein extraction were collected from the slaughter house with the kind assistance of Prof. Magnus Andersson. All animals were handled in accordance with the institutional animal care policies of the University of Turku, and all studies were approved by the local Animal Ethics Committee.

4.2   Genome wide scan (I)

The family structure of ISTS affected boars suggested autosomal recessive inheritance with full penetrance. The penetrance of the defect was further tested with litters of a carrier-carrier crossing and the outcome supported this assumption. All ISTS affected boars could be traced back to one common sire and most of them were closely related. Therefore, homozygosity mapping was used for a genome wide search of the defect. Homozygosity mapping is based on the fact that the adjacent region of the recessive disease locus will be homozygous by descent in inbred populations (Lander and Botstein. 1987). Affected and control pools used for whole genome scan contained DNA from 11 boars. Genome screening was performed using 228 fluorescently labeled autosomal microsatellite markers from the U.S. Pig Genome Coordination Programme with an average spacing of 10 cM. The genome scan with pooled samples was confirmed with experimental material obtained from 28 affected boars, which were also used for haplotype analysis. For linkage analysis parents and/or siblings were available for 24 boars. In total, 41 unaffected family members were sampled including sows (Fig. 7). To date, a total of 82 affected boars have been detected and samples for DNA extraction were available from 65 boars.
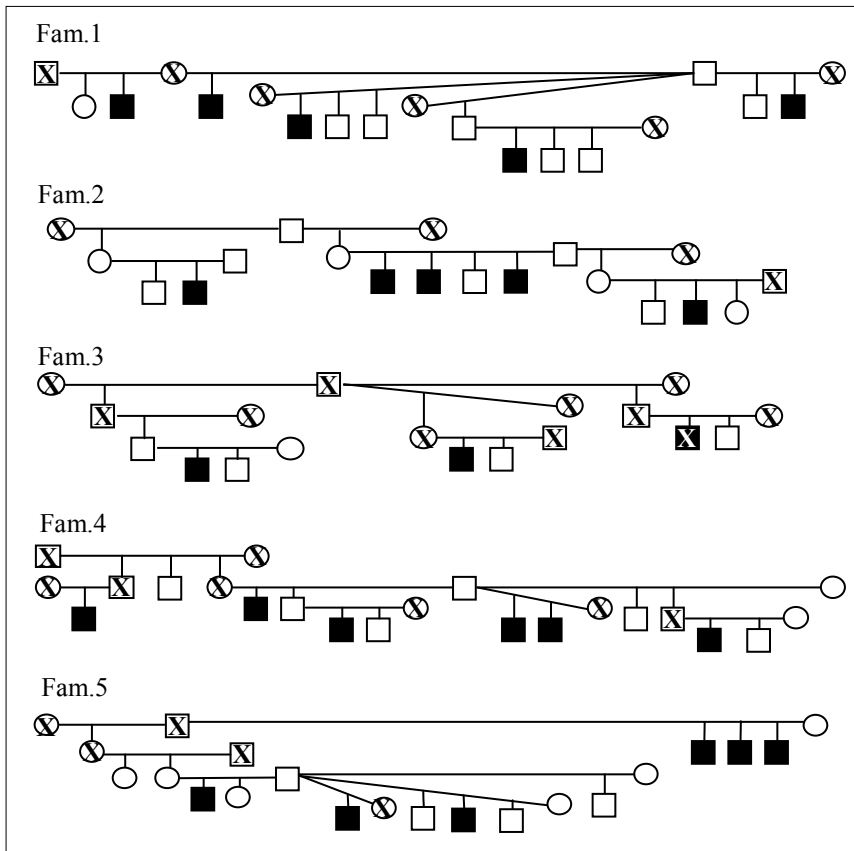
Figure 7. Schematic of family pedigrees used in the linkage study. ISTS affected boars are indicated by black boxes and individuals that were not genotyped with crossed circles and boxes. (Figure modified from I).

4.2.1 Statistical analysis

A χ^2-test was used for statistical analysis of the allele frequencies in the genome scan, and $P < 0.05$ following a Bonferroni-correction with the number of markers was considered significant. Linkage analysis was conducted with the Genehunter package (Kruglyak et al. 1996). An autosomal recessive mode of inheritance and complete penetrance were assumed for parametric linkage analysis. The frequency of the mutated allele was estimated to be 0.20 and the disease status in females was defined as unknown. Data from control animals was used to estimate allele frequencies. Map distances were obtained from the USDA MARC swine gene map.

4.3 Fine mapping (II)

For fine mapping, BAC clones (PigE BAC) from MCR Geneservice (http://www.hgmp.mrc.ac.uk, Anderson et al. 2000) were picked up by PCR screening with disease-associated markers on porcine chromosome 16. The selected BAC clones were isolated,

the BAC ends sequenced and compared with the human sequence database (http://www.ncbi.nlm.nih.gov/) in order to map the disease-associated area on the human map. Human gene sequences within this region were compared with the pig EST database (University of Aarhus, Faculty of Agricultural Sciences) and homologous porcine ESTs were sequenced in order to identify SNPs for further fine mapping. In total, 100 ISTS affected boars and family members were genotyped for 11 SNPs within three genes.

4.4   Mutation detection (II, III)

After fine mapping, a candidate gene approach was used for mutation detection. Porcine EST sequences for a candidate gene were used for primer design. The candidate gene mRNA and partial DNA were sequenced from an ISTS affected and a control boar in order to identify the causal mutation. Several ISTS affected, carrier and control boars were genotyped for 10 SNPs detected within the candidate gene transcript.

4.5   Southern hybridization analysis (II)

Porcine genomic DNA was digested with EcoRI, EcoRV and BamHI, and separated by electrophoresis on a 0.8% agarose gel in TBE buffer and transferred onto positively charged Hybond-NX membranes (Amersham Pharmacia). The membranes were hybridized with a DNA Probe labeled with EasyTides $[\alpha\text{-}^{32}P]$dCTP, 250 µCi (PerkinElmer). Hybridization and washings were carried out at 65°C according to standard protocols. Thereafter, membranes were exposed to x-ray films.

4.6   Marker and gene assisted selection (III)

During 2001 and 2005, a total of 1042 animals were tested with markers SW2411 and SW419 by Fabalab (http://www.faba.fi/). In year 2006, a new DNA-test was introduced for gene assisted selection. Primers within *KPL2* exon 30 and reverse primers within the beginning of the L1-insertion and beyond this insertion were used for genotyping in gene assisted selection (GAS). Furthermore, the presence of the *KPL2* insertion in other pig breeds was tested with genomic DNA samples of Finnish Landrace, Hampshire, Duroc/Hampshire cross breed, and Danish Yorkshire and Landrace boars.

4.7   RT-PCR and quantitative real-time PCR (II, IV)

For the analysis of *KPL2* gene expression in various tissues, samples from WT and ISTS affected boars were collected and stored in RNAlater buffer at -20ºC. For longer storage periods, the RNAlater buffer was discarded and samples were stored at -80ºC. Tissue samples of C57BL/6 mice were snap frozen in liquid nitrogen and stored at -80ºC.

Fragments corresponding to *KPL2* exons 7-8, 29-36 and 40-43 were used to examine the expression of different transcript variants of *KPL2* in the pig. *KPL2* exons 7-8 represent the *KPL2* variant 2, exons 40-43 variant 1 (Fig. 14) and exons 29-36 include the missing exon 30 in ISTS boars. In the mouse, *Kpl2* fragments corresponding to exons 3-7, 6-43 and 37-43 were examined in order to detect the occurrence of different variants. Total mRNA was amplified with RT-PCR and differences in transcript quantity were detected on agarose gels with ethidium bromide staining. Quantitative real-time PCR (qPCR) was used for a precise quantification of the relative mRNA transcript levels of *KPL2* in pig tissues. Two fragments of *KPL2* (exons 7-8 and 29-30) were analyzed using ribosomal 18S RNA as an internal reference gene. For studies in mice, RT-PCR ribosomal gene expression was used as a control.

4.8   Northern hybridization analysis (II)

Poly(A)-RNA was isolated using the Dynabeads DIRECT mRNA kit (Dynal, Invitrogen) following the manufacturer's instructions. Each RNA sample was denatured by boiling for 10 min and loaded onto a 1% agarose-formaldehyde gel. RNA was transferred to positively charged nylon membranes using the NorthernMax kit (Ambion). The probe corresponding to *KPL2* exons 3–7 was radioactively labeled with the Nick Translation System (GIBCO_BRL) using [α-^{32}P]dCTP (Amersham Pharmacia).

4.9   *In situ* hybridization (IV)

Testis samples from C57BL/6 mice were fixed in 4% paraformalehyde (PFA, EM-grade) and 0.2% sucrose, frozen at -80ºC and sliced into 10 µm sections. In order to localize the *Kpl2* mRNA products in the mouse testis two Locked Nucleic Acid (LNA) probes (Exiqon) corresponding to exons 6 and 43 were used for mRNA detection and a scrambled probe (Exiqon) was used as a negative control. Probes were labelled with a DIG tailing kit (Roche Applied Sciences) and hybridized over night at 37ºC. Signals were detected using the tyramide signal amplification system (PerkinElmer) according to the manufacturer's instructions.

4.10 Western hybridization analysis (IV)

Various tissue samples from C57BL/6 mice and WT and ISTS pigs were collected for protein extraction and stored at -80ºC. After extraction, the protein content was measured. Samples were separated by SDS-PAGE and blotted to a nitrocellulose membrane. Antigen-antibody complexes were detected by incubation with the anti-rabbit secondary antibody (horseradish peroxidase-conjugated, GE Healthcare) and located with the

ECL Plus Western blotting detection system (GE Healthcare) and exposed to a film thereafter.

4.11 Immunohistochemical analysis (IV)

Testis samples from C57BL/6 mice were collected and squash preparations, PFA-fixed and cryosections were prepared as described in paper IV. Spermatozoa from the caput, corpus and cauda epididymis and the vas deferens were washed in PBS, spread on a slide and stored at -80°C. Testis sections or spermatozoa were incubated with mouse monoclonal anti-α-tubulin (1:150, Cell Signalling Technology), rabbit monoclonal anti-AKAP4 (1:200, BD Biosciences), polyclonal anti-IFT20 antibody (1:300, a generous gift from Prof. Pazour, University of Massachusetts Medical School, USA), polyclonal anti-GAPDHS antibody (1:500, a generous gift from Prof. Kamp, Molecular Physiology Section, Johannes Gutenberg-University, Germany) or rabbit polyclonal anti-KPL2 (1:200, Medprobe) or rabbit anti-IgG (used at the same concentration with antibodies as the negative control). Peptide blocking of KPL2 antibody was also used as a negative control for KPL2 protein localizations. Mitotracker (200 nM, Invitrogen) was used for detection of mitochondria and Lectin Helix pomatia agglutinin (HPA) Alexa Fluor 488 Conjugate (Molecular Probes) for staining of the Golgi complex. Alexa Fluor 594 goat anti-rabbit IgG or Alexa Fluor 488 goat anti-mouse IgG (1:500, Molecular Probes) were used as secondary antibodies and nuclei were stained with 4',6-diamidino-2-phenylindole (Dapi, Sigma Aldrich).

4.12 Protein interaction studies (IV)

A yeast two-hybrid screen was used to detect KPL2 interacting proteins. Three KPL2 fragments KPL2-N (1-516aa), KPL2-M (429-924aa) and KPL2-C (1333-1823aa) corresponding to predicted domain structures (Fig. 20) were used to construct the bait plasmid in the pGBT9 expression vector. These bait plasmids were used to screen human brain Matchmaker cDNA library (Clontech Laboratories, Inc.) co-transformed into yeast strain PJ69-4 using the LiAc-PEG method (Gietz and Woods. 2002). The human brain cDNA library was used, since no testis cDNA libraries were available at that time. The human brain Matchmaker cDNA library was cloned into pGAP10 (hunter plasmid) and transformed into *E. coli*. Plasmids were isolated from yeast cells containing plasmids that support growth on selective media (Hoffman and Winston. 1987) and sequenced using the BigDye®Terminator v.3.1 Cycle sequencing Kit (PE Applied Biosystems). The inserted sequences were identified by BLASTn searches against GenBank. Interactions were also examined with deletion constructs of the interacting KPL2-C. Four deletion constructs of KPL2 were produced from porcine testis; KPL2-C, KPL2-C1 (1324-1676aa), KPL2-C2 (1462-1676aa) and KPL2-C3 (1671-1822aa). KPL2 constructs

and the entire open reading frame of IFT20 were obtained by PCR from the pig testis mRNA. Fragments were subcloned into yeast two-hybrid expression vectors pGBT9 and pGAD10. Transformed yeast cells were grown on synthetic complete double dropout plates (Trp and Leu) and protein-protein interactions were selected on triple dropout plates (Trp, Leu and Ade).

The interaction detected by yeast two hybrid analysis was further confirmed with co-immunoprecipitation (coIP) of KPL2 and IFT20. Tissue samples of C57BL/6 mice and WT and ISTS pigs were extracted and immunoprecipitated (IP) with the KPL2 antibody or rabbit IgG. IP samples were separated by 15% SDS-PAGE and blotted to a nitrocellulose membrane. The membrane was incubated overnight with IFT20 antibody and detected as described for Western blotting analysis.

4.13 Bioinformatics (I-IV)

DNA, mRNA and protein sequences were obtained from the NCBI database (http://www.ncbi.nlm.nih.gov/) and EntrezGene predicted the exon-intron boundaries. The Blast and ClustalW programmes were used to analyze similarities and to align nucleotide or protein sequences. The porcine KPL2 protein sequences were translated from the cDNA sequence by the Translate-programme and protein functional domains were predicted with the InterProScan, Pfam, Smart and Prosite programmes. ProScan, ReapeatMasker and splice site prediction were used for analysis of the *KPL2* L1-insertion.

Table 2. Bioinformatic tools used in the study and their function and information source.

Programme	Function	Source
Translate	DNA -> protein	http://www.expasy.ch/tools/dna.html
Blast	Similarity searches	http://www.ncbi.nlm.nih.gov/blast/Blast.cgi
ClustalW	Sequence alignment	http://www.ebi.ac.uk/Tools/clustalw/index.html
ProScan	Promoter scan	http://bimas.dcrt.nih.gov
RepeatMasker	DNA repeat searches	http://www.repeatmasker.org
	Splice site prediction	http://www.fruitfly.org/seq_tools/splice.html
InterProScan	Pattern and profile searches	http://www.ebi.ac.uk/InterProScan/
Pfam	Pattern and profile searches	http://www.sanger.ac.uk/Software/Pfam/
Prosite	Pattern and profile searches	http://www.expasy.ch/prosite/
Smart	Pattern and profile searches	http://smart.embl-heidelberg.de/
EntrezGene	Exon-intron boundaries	http://www.ncbi.nlm.nih.gov/sites/entrez?db=gene

5.   RESULTS

5.1   Genome wide scan mapped ISTS to porcine chromosome 16 (I)

To identify the ISTS associated loci, DNA from 11 ISTS affected and control boars were pooled to reduce sample numbers. These two DNA pools were used for the initial genome screen. This genome wide scan highlighted several markers exhibiting increased homozygosity in the ISTS-affected DNA-pool compared with the control pool. Individual DNA samples were genotyped with these markers to elucidate actual allele frequencies. Only one marker (SW2411) in porcine chromosome 16 showed a difference (P<0.001) in allele distribution between affected and control individuals. Therefore, all available adjacent markers were analysed. Increased homozygosity in affected boars was also seen for markers SW419 and SW1035. Five markers (SW742, SW1035, SW2411, SW419 and SW1645) covering 16 cM around the ISTS-associated region were genotyped with DNA samples of ISTS-affected boars and their available relatives for linkage analysis (Fig. 7). Linkage analysis by Genehunter-programme confirmed an association of the chromosome region with ISTS, as indicated by a maximum LOD score of 7.7 at marker locus SW419 (Fig. 8). The 95% confidence interval (1 LOD drop-off criterion) spans a region of 6 cM around the marker (Fig. 8). Only one ISTS-affected boar was heterozygous for marker SW419 and several recombinations were detected between the ISTS loci and other markers. Based on the haplotype data, the ISTS mutation lied between markers SW2411 and SW419, which reduced the confidence interval to a 3 cM region proximal to SW419. Furthermore, marker S0006 was located within this 3 cM region, but it was not informative for the Finnish Yorkshire population.
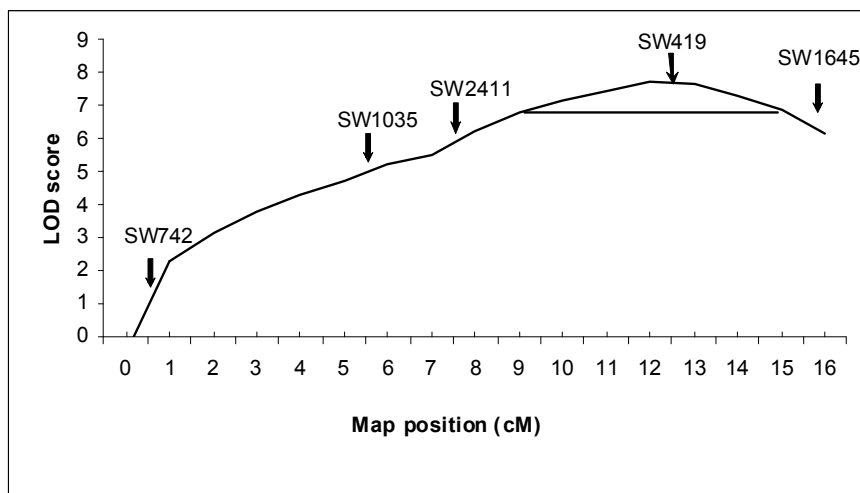

Figure 8. Linkage analysis located the ISTS associated region by 95% confidence interval to 6 cM around marker SW419 in porcine chromosome 16 (solid line). Markers used in the linkage analysis are shown with arrows and the map position is indicated on the x-axis. (Figure from I).

5.2 Fine mapping decreased the disease-associated region to 1.2 Mbp (II)

Porcine BAC clones were collected with markers SW2411, SW419 and S0006. BAC end sequences were used for BLASTN searches against the human NCBI database. The area between SW419 and S0006 was located within a 2 Mbp region on human chromosome 5p13.2. SNPs from porcine ESTs corresponding to human genes within this region were found in *AMACR* and *RAI14* (Fig. 9). A recombination in two affected boars between the ISTS defect and *RAI14* reduced the disease-associated region to 1,158 Kbp in the human map containing eight annotated genes (*RAI14, FLJ25439, RAD1, BRIX, LOC134218, AGXT2, PRLR* and *FLJ25395/FLJ23577*, Fig. 9).
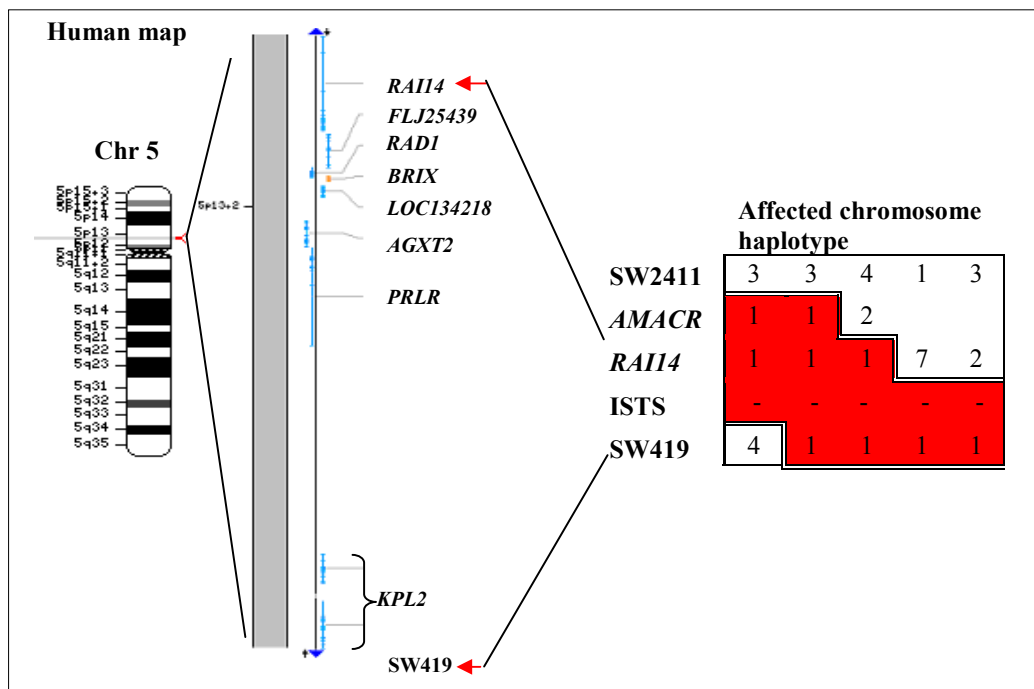
Figure 9. Comparative mapping located the ISTS-associated area on human chromosome 5p13.2. Fine mapping with porcine SNPs within genes *AMACR* and *RAI14* reduced the disease-associated region to 1,158 Kbp on human chromosome 5, which contains only eight annotated genes. Based on porcine BAC sequence homology with the human genome, porcine marker SW419 is located near the 3' end of *KPL2*.

5.3 Sequencing of *KPL2* gene revealed an L1 insertion (II-III)

The human hypothetical protein FLJ23577 had a 79.4% (nt%ID) homology to the rat KPL2 (also kown as sperm flagellar 2, SPEF2), which is highly expressed in the seminiferous tubules of the testis (Ostrowski et al. 1999). In addition, it appeared that the hypothetical gene *FLJ25395* was also homologous to *Kpl2*. The testis cDNA of *KPL2*

was sequenced from a control and an ISTS-affected boar, allowing 10 SNPs and a lack of exon 30 to be identified. All of the 10 SNPs were found to be homozygous for both alleles in unaffected boars, suggesting that the lack of exon 30 is the underlying cause for the ISTS defect. Furthermore, the exon 30 sequence was present in the DNA of affected boars, which implicated that the causal mutation lies within the noncoding sequences of *KPL2*.

KPL2 intron 29 (3305 bp) and the beginning (1500 bp) of intron 30 were sequenced from a control and an ISTS-affected boar DNA. Three SNPs were found within these sequences and no PCR product was produced from the beginning of intron 30 for the ISTS-affected boars. A large insertion was detected 168 bp from the beginning of intron 30 of affected boars with Southern blotting. PCR with specific primers adjacent to the insertion revealed an approximate 9000 bp insertion unique to ISTS-affected boars (Fig. 10). This appears to be the causal mutation for ISTS defect.
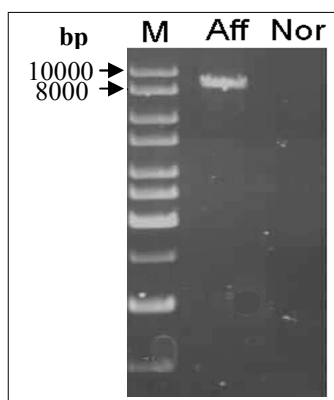

Figure 10. Line-1 insertion within the *KPL2* gene is only present in ISTS-affected (Aff) individuals compared with control boars (Nor) as shown by PCR with *KPL2* intron 30 specific primers. The size of the PCR fragment including the insertion is approximately 9000 bp as indicated by the molecular marker (M). (Figure adapted from II and III)

Sequencing of the insertion (EF599954) showed that a 7878 bp fragment was present in *KPL2* intron 30 of affected boars. Analysis of the insertion sequence revealed a full-length long interspersed nuclear element-1 (Line-1, L1) retrotransposon, containing typical L1 domains such as promoter region, ORF1 and ORF2 (Fig. 18). Analysis of the insertion target sequence in *KPL2* intron 30 revealed regions of conserved sequences on both sides of the insertion site, which may contribute to aberrant splicing of *KPL2*. In addition, a cryptic 3' splice acceptor site associated with a pyrimidine-rich sequence and the consensus branch site motif were identified in the intron sequence.

5.4   L1 insertion alters the splicing pattern of *KPL2* (II)

Expression studies showed that the L1 insertion affects *KPL2* splicing in two ways; the majority of ISTS mRNAs are lacking exon 30, but in some cases exon 30 is present including part of the intron 30 and beginning of the insertion (Fig. 11). In both cases the altered splicing pattern results in premature stop codons, which truncate the protein at

residues 1403 and 1487, respectively, from a total of 1812 amino acids. PCR amplification of cDNA across base pairs 3978-4466 (exons 29-36) produces a fragment of 488 bp in control boars and a fragment of 258 bp in ISTS-affected boars. A less abundant fragment of 999 bp was also detected in two ISTS-affected boars. Sequencing of the fragments showed that exon 30 (230 bp) was missing in the shorter fragment, but present in the longer fragment in combination with part of intron 30 (59 bp preceding the insertion) and the beginning of the insertion (452 bp).
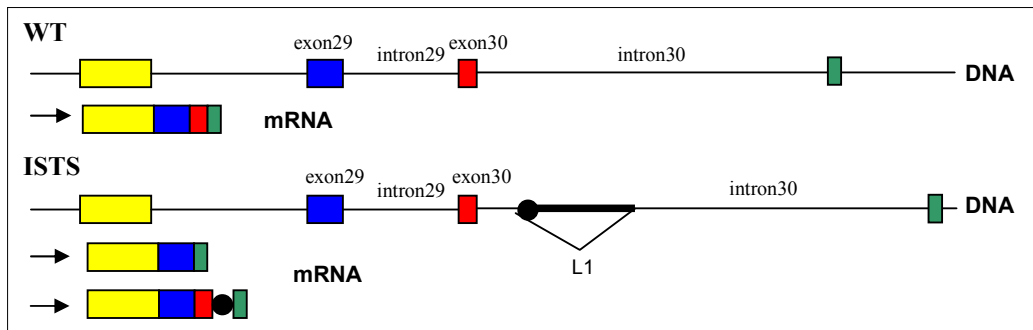
Figure 11. Alterations in *KPL2* exon 30 splicing in ISTS-affected boars. In most transcripts exon 30 is skipped, but in a few cases exon 30 is included together with part of intron 30 and the L1-insertion sequence (black circle).

Comparison of expression in tissue samples of ISTS-affected and normal boars indicated that expression of *KPL2* exons 7-8 was primarily down-regulated in the testis (3.8-fold), while expression in the trachea, lung and liver appeared less affected. Furthermore, the expression of exons 29-30 was decreased 15-fold in the testis and 3-fold in the trachea of ISTS-affected boars relative to normal individuals.

5.5   Genetic testing of ISTS defect (III, unpublished)

In order to reduce the frequency of ISTS in the Finnish Yorkshire population, the first DNA-test for MAS of the ISTS defect was introduced in 2001. Since this time it has been made available to Finnish pig breeders by Fabalab. The test was based on a two marker haplotype (SW2411 and SW419) and used within analyzed pedigrees. In 5% of all tested animals the disease status was not definable (ND) using the marker haplotype, since the disease associated haplotype was also present in unaffected animals. In total 696 unaffected, 268 carrier, 27 affected and 51 ND animals were tested between the years 2001 through to 2005. In 2001, the carrier frequency was as high as 36%, while implementation of MAS reduced this to 18% by the end of 2005 (Fig. 12).
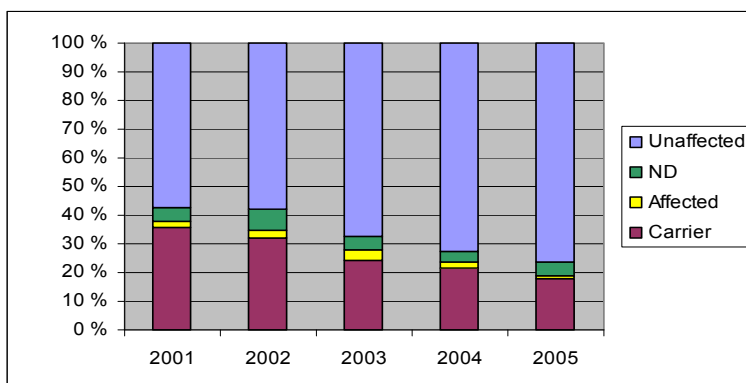
Figure 12. Frequencies of different ISTS genotypes detected by the two marker haplotype DNA test in Finnish Yorkshire pigs during the period 2001 to 2005. The carrier frequency was reduced from 36% to 18% using MAS. For about 5% of animals tested it was not possible to determine the disease status (ND) using the two marker haplotype.

Due to inaccuracies of the marker based test, a more precise test was required for selection against ISTS. This was enabled by the identification of the disease causing mutation. For gene assisted selection a forward primer within *KPL2* exon 30 and a reverse primer within the beginning of the insertion (Fig. 13) were used for the detection of ISTS affected chromosomes. The same forward primer and a reverse primer in intron 30 after the insertion site were used as a marker for unaffected chromosomes.
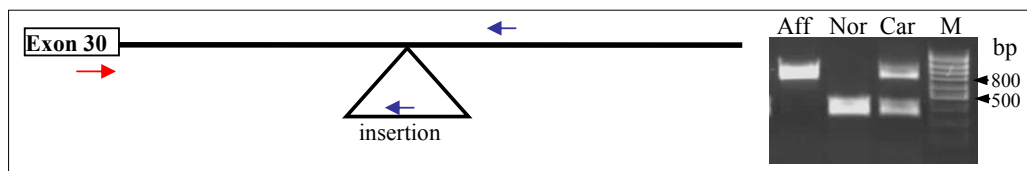

Figure 13. The PCR based test used for gene assisted selection of ISTS. The forward primer within *KPL2* exon 30 is indicated by a red arrow and reverse primers within the insertion and intron 30 just after the insertion by blue arrows. In ISTS-affected animals (Aff) only a fragment of 863 bp is detected. In samples of unaffected animals (Nor) a fragment of 354 bp is present. Both fragments are detected in ISTS carrier animals (Car). M = molecular marker.

The insertion was found to be homozygous only in ISTS-affected boars and heterozygous in carrier pigs (Fig. 13). The DNA-test for GAS was first introduced by Fabalab in 2006. Furthermore, the mutation appears to be specific to the Finnish Yorkshire, since the *KPL2* insertion has not been detected in samples from individuals of the Duroc, Hampshire, Landrace or Danish Yorkshire breeds.

5.6 *KPL2* is differentially expressed (II, IV)

Expression of different exon combinations of *KPL2* were examined with RT-PCR in pig and mouse tissues and also during the first wave of mouse spermatogenesis. *KPL2* appeared to be differentially expressed in various tissues, whilst species differences were also detected. In the human, sequences of possible transcript variants of *KPL2* have been deposited in the NCBI genbank (Fig. 14). In addition to the full-length variant 1, several full insert sequences with varying exon content indicate complex transcription of *KPL2*. Several of these variant mRNAs contained retained genomic sequences, which are probably not translated.
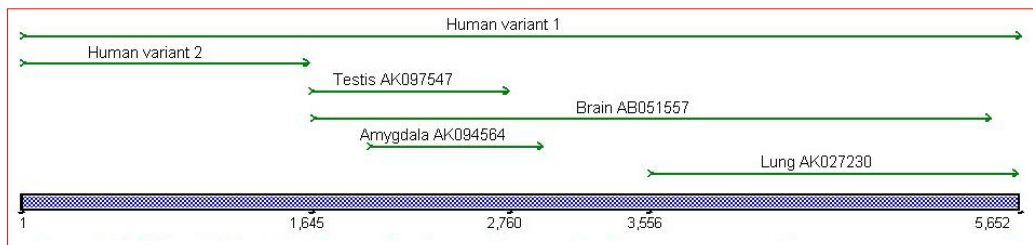

Figure 14. Possible human *KPL2* transcript variants in the NCBI database. Two different isoforms (1 and 2) have been identified in the human as well as various full-length transcripts. Only mRNA sequences corresponding to the *KPL2* variant 1 were included in the alignment.

5.6.1 Long *KPL2* variant is mainly expressed in the porcine testis (II, unpublished)

Expression of two fragments corresponding to *KPL2* variant 1 (NM_024867) and 2 (NM_144722) were determined in the porcine testis, trachea, lung and liver with qPCR. In addition, samples of the kidney and heart were analysed for *KPL2* expression on agarose gels. In normal boars, the expression of *KPL2* exons 7-8 (short form) were 2.3-, 6-, and 12-fold lower in the trachea, lung, and liver, respectively, compared with expression in the testis. *KPL2* exons 29-30 (long form) were expressed mainly in the testis and at a lower level in the trachea (4.3-fold). The testis specific expression of the long variant (variant 1) of *KPL2* was also confirmed by Northern Blotting. On an agarose gel, *KPL2* expression in the kidney was comparable to that in the liver. No expression was detected in heart tissue.

Expression patterns of *KPL2* exons 3-7 and 37-43 were studied in the testis, lung, brain, kidney, liver and heart by RT-PCR (unpublished results). *KPL2* exons 3-7 were predominantly expressed in the testis, lung and kidney, where two variants were present. The shorter PCR fragment lacked exon 4, which was more abundant in the lung and kidney compared with the testis (Fig. 15, 1A). *KPL2* exons 37-43 were expressed mainly in the testis, but also in the lung, and to a small extent in the kidney (Fig. 15, 2A).

5.6.2 Long *Kpl2* variant is testis specific in the mouse (IV)

Various fragments of *Kpl2* were also examined for possible expression in mouse tissues. *Kpl2* was found to be expressed in the testis, lung, brain, kidney and liver, but not in the heart. *Kpl2* exons 6-43 were expressed exclusively in the testis. Exon 4 also appeared to be testis specific. A *Kpl2* fragment containing exons 3-7 (except exon 4) was expressed in the lung, and at much lower levels in the brain, kidney and liver (Fig. 15, 1B). However, *Kpl2* exons 37-43 were expressed in all examined tissues, other than the heart (Fig. 15, 2B).
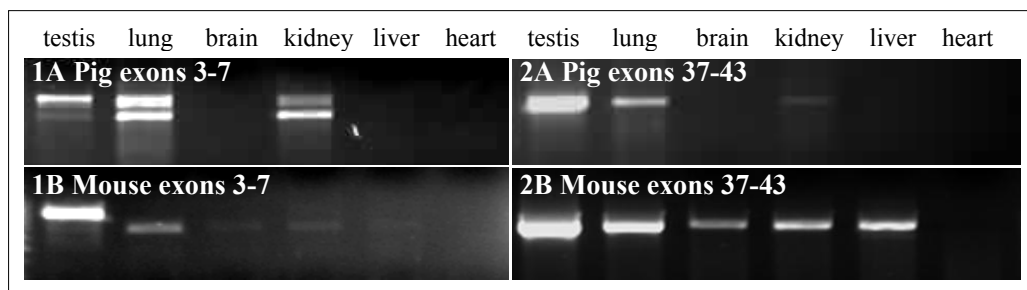
Figure 15. Differential expression of *KPL2* in porcine (A) and murine (B) tissues. RT-PCR of *KPL2* exons 3-7 (1) and exons 37-43 (2). Some differences in *KPL2* expression between species appear to exist.

5.6.2.1 *Kpl2* is differentially expressed during spermatogenesis

Differential expression of *Kpl2* was detected at different stages of the first wave of murine spermatogenesis. *Kpl2* exons 6-43 were expressed initially after PND 21, whilst exons 3-7 were expressed starting on day 28. In addition, exons 37-43 appeared to be weakly expressed from PND 7 with expression increasing from PND 21.

5.6.2.2 *Kpl2* mRNA localizes to spermatocytes and spermatids

Two probes for murine *Kpl2* exons 7 and 43 resulted in a similar expression pattern in late spermatocytes and spermatids. Probes were first detected at stage VII late spermatocytes with increasing intensity that peaked in stage XII spermatocytes. The *Kpl2* signal was also relatively high in step 1-7 spermatids, but disappeared at step 8. Although exons 37-43 were expressed in young animals with only spermatogonia in the testis, no localization was detected in spermatogonia. This may reflect the low amount of this mRNA variant compared with the much higher abundance of various *Kpl2* variants in late spermatocytes and spermatids. Furthermore, *Kpl2* appeared also to be expressed in stage VIII-XI SCs.

5.7 KPL2 protein localizes to testicular cells and the sperm tail (IV)

5.7.1 Long isoform of KPL2 is depleted in ISTS-affected testis

The long isoform of KPL2 was detected in the sample of WT boar testis, highlighting that the lack of this form of KPL2 is responsible for the ISTS defect. KPL2 antibody

also detected two short forms of KPL2 in the testis of WT and ISTS boars. In immunofluoresence assays similar staining patterns of KPL2 were detected in the testis preparations of WT and ISTS boars, with the implication that these KPL2 localizations are probably due to the short isoforms of KPL2.

In squash preparations of the pig seminiferous tubules, KPL2 localized to the Golgi complex of round spermatids of WT and ISTS boars. The Golgi localization was confirmed with Golgi marker lectin HPA conjugate. KPL2 was detected mainly around the HPA staining, indicating that KPL2 appears to be mainly present in the trans-Golgi compartment (Fig. 17A). In cryosections, KPL2 antibody stained the SC cytoplasm and spermatid crypts of WT testis section, whilst reduced staining was detected in the ISTS-affected testis.

5.7.2 KPL2 localizes in murine germ and Sertoli cells

In the mouse, expression of a long KPL2 isoform was demonstrated by western blotting and was found to be exclusively expressed in the testis at PND 21. Various minor protein products were also observed. Most of these minor protein bands disappeared by peptide blocking indicating that they are specific KPL2 products. However, these bands may also be products of protein degradation. The mRNA expression results suggest the presence of different transcript variants of *Kpl2* in the testis and as such various protein isoforms also probably exist.

KPL2 protein products were examined in cryosections, PFA-fixed sections, staged squash preparations and drying down slides of samples from the WT C57BL/6 mouse testis. In PFA-fixed and cryosections the staining first appeared in late spermatocytes (stages VIII-XII) and later in the residual body of step 16 spermatids, but no staining was detected in round spermatids (Fig. 16A). In squash preparations and drying down slides, intense KPL2 staining was detected in SC cytoplasm and spermatid crypts. Prior to elongation spermatids form bundles (stage IX-X) and KPL2 localizes around the spermatid heads, which appeared to be connected to SC by the SC cytoplasm (Fig. 17C). SC cytoplasm staining in stages (VIII) XI-I moved to spermatid crypts in stages I-VII (VIII). The KPL2 signal was also seen as a dense spot outside the nucleus (Fig. 17B) possibly representing the Golgi complex (unpublished data).

5.7.3 KPL2 localizes in the pig sperm tail fibrous sheath

During spermiogenesis in the pig, KPL2 was not detected in elongating spermatids. In epididymal sperm of WT boars, KPL2 was localized in the principal piece of the sperm tail in caput spermatozoa, but depleted during epididymal passage. In ISTS sperm, weak KPL2 staining was detected along the short tail while the staining pattern was constant in the caput, corpus and cauda. This expression pattern was also supported by the results of Western blot of KPL2 protein in the testis and in epididymal sperm.

5.7.4 In murine sperm KPL2 resides in the tail midpiece

In the mouse, the KPL2 protein was first detected in the manchette of step 9-12 spermatids (Fig. 17D), and thereafter in the basal body and neck region at steps 13-14. At steps 15-16, KPL2 became evenly distributed along the midpiece of the sperm tail (Fig. 21). Accumulation of KPL2 in the sperm midpiece was correlated with mitochondrial sheath formation (Fig. 16B). However, most of KPL2 was detected outside the mitochondria in granulated manner. The FS protein AKAP4 first appeared at step 11 before KPL2 staining in the sperm tail.
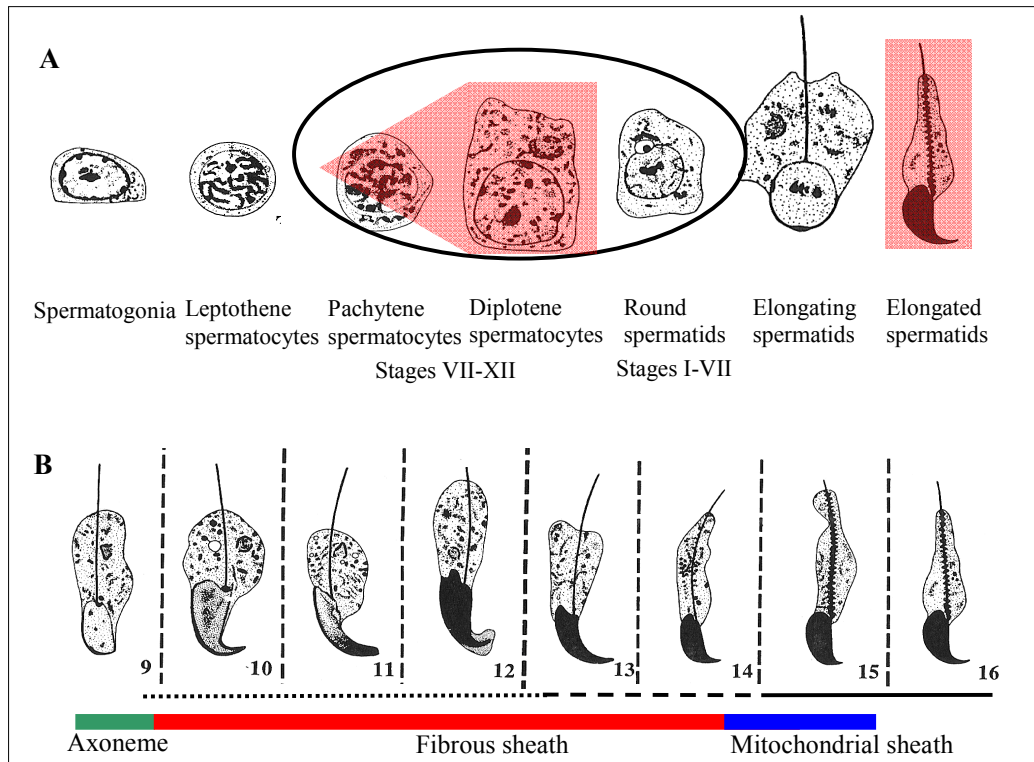
Figure 16. *KPL2* mRNA and protein localizations during murine spermatogenesis. A. Transcription and translation of KPL2 were highly correlated and started in pachytene spermatocytes. *Kpl2* mRNA was present until sperm tail elongation started at step 8. KPL2 protein was detected in late spermatocytes and in the residual body of elongated spermatids. *Kpl2* mRNA expression is represented by a circle and cytoplasmic protein expression is indicated by the red background. B. KPL2 protein was also detected in the manchette of step 9-12 elongating spermatids (dotted line) moving to the basal body and neck region at steps 13-14 (dashed line) and finally to the mid piece of the sperm tail in elongated spermatids (solid line). Formation of sperm tail structures is indicated with coloured bars; axoneme in green, FS in red and MS in blue.

Localization of KPL2 immunostaining changed during epididymal passage of spermatozoa. In most of the caput sperm, KPL2 staining was comparable to that in the testis. However, unstained regions along the midpiece were also observed. In corpus sperm the scattering of the staining pattern was clearer and tended to concentrate in the

distal part of the midpiece. In spermatozoa from the cauda epididymis and vas deferens, KPL2 staining was only detected in the distal midpiece section (Fig. 21).
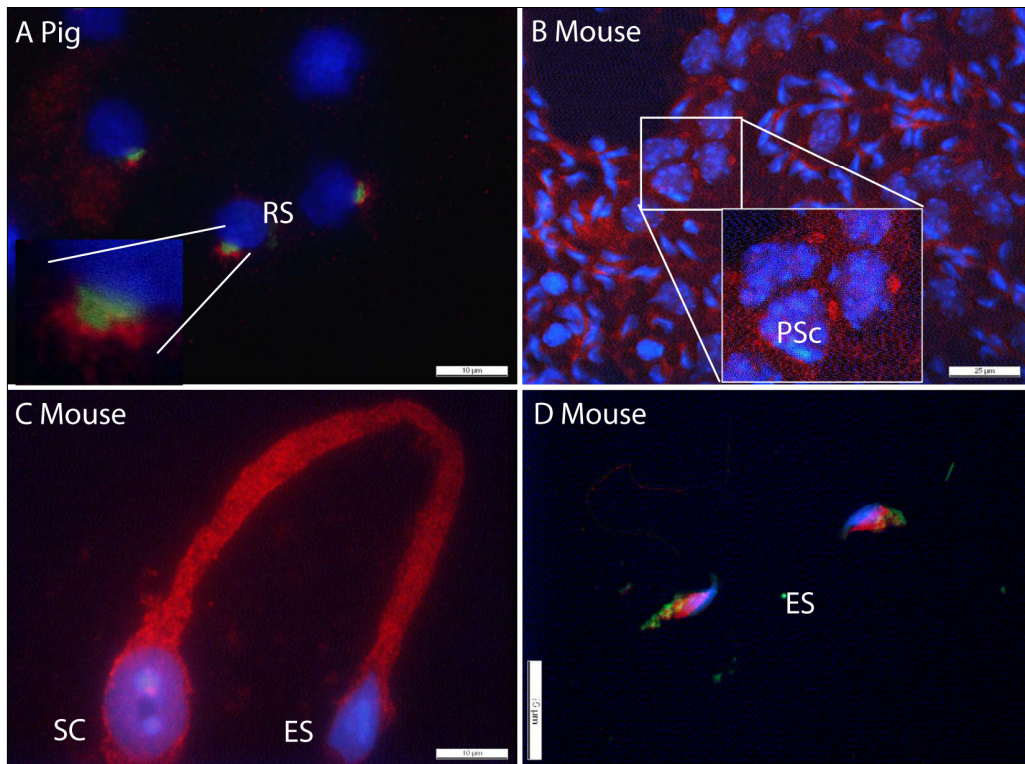

Figure 17. KPL2 protein is present in the Golgi complex, SCs and the sperm manchette. A. Co-localization of KPL2 (red) and Golgi marker HPA (green) in porcine round spermatids (RS). KPL2 is predominantly located in the trans-Golgi compartment. B. Localization of KPL2 as a spotted structure in mouse stage X-XII late spermatocytes (pachytene spermatocytes, PSc). C. In the mouse, KPL2 staining was detected in the SC cytoplasm connecting the SC to elongating spermatid (ES) heads. D. Prior to MS formation, KPL2 (red) is located in the mouse sperm manchette. No clear localization in the axoneme was detected. Mitochondria are indicated by the green fluorescence of the Mitotracker, KPL2 staining by the red fluorescence and nuclei are highlighted by the blue Dapi staining.

5.8   KPL2 interacts with IFT20 (IV)

In order to further elucidate the role of KPL2, a yeast two hybrid screen was used to identify possible interacting partners. In the initial screen of human brain cDNA library a possible KPL2 interaction with the intra flagellar transport protein IFT20 was detected. The library screen indicated a novel interaction between the C-terminal part of KPL2 (KPL2-C) and IFT20. Deletion constructs of KPL2-C were generated from the pig testis and tested against IFT20 in order to further characterize the interaction. Constructs KPL2-C and KPL2-C1 were capable of interacting with IFT20, indicating that the region

consisting of amino acids 1324-1462 in KPL2 is important for the interaction between IFT20 and KPL2.

Interaction between KPL2 and IFT20 was also supported by coIP of the murine and porcine testis tissues. In both species KPL2 immunoprecipitated lysates contained IFT20 protein. No clear differences in KPL2/IFT20 interaction were present between normal and ISTS boars indicating that this interaction is not severely affected by the ISTS mutation. No interaction was detected with a negative control and the similar protein content within each lane was confirmed by IgG.

Comparable localizations of KPL2 and IFT20 protein products further support their interaction. Both proteins localize in the manchette of step 9-12 spermatids and relocate to the basal body at steps 13-14 (Fig. 21). KPL2 and IFT20 appear to be also present in the Golgi complex in stage VIII-XII mouse spermatocytes (data not published); however this observation requires further examination. In addition, IFT20 was also detected in the Golgi complex of step 1-8 spermatids in drying down preparations.

6. DISCUSSION

6.1 The impact of ISTS on Finnish pig breeding and developing a long-term solution

The ISTS defect became a significant economic burden to the Finnish pig breeding industry at the end of 1990s, when several boars were found to be affected. All ISTS-affected boars were closely related and the defect seemed to be inherited as an autosomal recessive disorder enabling a genetic approach to resolve the underlying cause of the symptoms. The ISTS defect appears to be inherited from a few carrier boars to all affected animals and it could be traced back to one common ancestor. Thus, the propagation of the ISTS defect is a good example of the negative effects of inbreeding in closed populations. In order to develop a DNA-test for MAS and thereafter for GAS, the gene hunt was initiated by a genome wide scan of affected and control DNA pools. Marker- and gene-assisted selection enables the elimination of ISTS-affected piglets. Furthermore, asymptomatic homozygous sows can also be identified and the carrier information used for selection purposes. Early removal of affected animals offers the advantage of significantly reducing the cost of pig breeding programmes.

6.1.1 Generating MAS and practical implementation

Homozygosity mapping proved to be a powerful tool for the genome wide search of the ISTS locus. Although some false positive results were picked up from the initial screen with pooled samples, genotyping of individual samples provided a definitive result for further fine mapping. The ISTS-associated genomic region was located to porcine chromosome 16 between markers SW2411 and SW419 (I). Although marker SW419 was only heterozygous in one affected chromosome, the adjacent (distance 3 cM) marker SW1645 showed no association with the ISTS defect, indicating a recombination hot spot between these two markers. This two marker haplotype enabled MAS within the Finnish Yorkshire pig population to be implemented in 2001, offering the opportunity to remove ISTS-affected and carrier animals from the breeding programme. While the carrier frequency was clearly reduced with MAS, the full potential of the test was not realized. Affected/carrier individuals may also contribute positively to production traits and therefore carriers are still used for breeding purposes. This is also supported by the rapid proliferation of the defect during the 1990's. Even though MAS determined the disease status for 95% of tested animals, a more precise test was required. Inaccuracies in the test arise from different ISTS-associated haplotypes being present in unaffected animals. In addition, parental haplotype information was also required for the determination of disease status.

6.1.2 Effective fine mapping using human sequence information

Since the porcine genome sequence is not available, comparative mapping of the pig and human sequences was exploited in the discovery of the ISTS responsible gene. In order to detect genes within the ISTS-associated region comparative mapping with the human genome was shown to be an effective method. Three markers (SW2411, S0006 and SW419) were used to construct a partial porcine BAC-contig. The conserved nature of non-expressed sequences between species enabled comparison of BAC-end sequences with the human genome. The region between markers S0006 and SW419 was located on human chromosome 5. The human gene sequences within this region were compared with porcine ESTs (database in University of Aarhus, Faculty of Agricultural Sciences). Several SNPs within these ESTs were heterozygous in a few ISTS-affected boars defining the location of the causative gene within 1,158 Kbp on the human map (II, Fig. 9). Since the ISTS mutation appears to have arisen 10-15 generations ago, the region identical by descent in affected animals was assumed to be large. The high number of recombinations around the ISTS locus is evident, suggesting altered recombination rates in ISTS-carrier animals. However, the cause for altered recombination rate remains unclear.

Although fine mapping reduced the disease-associated region to eight annotated genes, mutation detection required the selection of candidate genes. A good candidate gene was identified as a hypothetical gene in the human map corresponding to the *Kpl2* gene in the rat. *KPL2* is expressed in tissues containing cilia-like structures suggesting a role for this gene in ciliogenesis (Ostrowski et al. 1999)**.** Sequencing of the *KPL2* cDNA showed two abnormal splice products in ISTS affected boars. The majority of the *KPL2* transcripts in affected boars lacked exon 30, whereas a minor fraction retained exon 30, but also included intronic as well as insertion sequences (II). Retention of intron and L1 sequences in a minor proportion of *KPL2* transcripts appeared to be caused by the activation of a cryptic splice acceptor site (III). Both abnormal splicing events lead to disrupted reading frames generating premature translation stop codons and truncated protein products. The amount of *KPL2* transcripts (qPCR, exons 7-8) were reduced in affected testicular tissue (II), possibly as a result of mRNA degradation by nonsense-mediated decay of transcripts containing premature termination codons. In addition, no protein products corresponding to these truncated *KPL2* forms were detected in Western blot analysis (IV), with the implication that the majority of the incorrectly spliced mRNA is degraded prior to translation.

6.1.3 Characterization of the causal insertion

Since the *KPL2* exon 30 was present in the DNA of ISTS-affected boars and no obvious reasons for exon skipping were detected in the coding region of *KPL2*, the intronic regions around exon 30 were sequenced. All SNPs found within introns, as well as in exons of *KPL2* were also homozygous for the disease associated allele in normal boars

further supporting the hypothesis that the ISTS mutation is a recent event. The cause for the aberrant splicing pattern was found within *KPL2* intron 30 and shown to be a large insertion with a high degree of homology to L1 retrotransposons (III).

Line-1 retrotransposons are the most abundant replicating repetitive elements in the mammalian genome. L1 replicates through transcription and reverse transcription generating a new copy at a new location in the genome, which can lead to mutagenic effects (Han and Boeke. 2005). Although the vast majority of the L1 insertions within the genome are inactive due to 5' end truncation or incapacitating mutations, the insertion in porcine *KPL2* gene appears to be an active L1. This includes all the characteristic L1 features such as a bidirectional promoter, 5'UTR monomer repeats, ORF1 and ORF2, providing strong support for the retrotransposon being functional and retrotransposition-competent. Furthermore, a canonical polyadenylation signal is found in the 3'UTR, followed directly by a polyA stretch and a direct repeat of 14 bp at both ends of the insertion arising from target-sequence duplication generated by target-primed reverse transcription (Babushok and Kazazian. 2007, III, Fig. 18). In the mouse, monomer repeats have been shown to increase L1 activity (Severynse et al. 1992), which supports the assumption of a highly active role for this porcine L1. In addition to the sense promoter that controls the expression of the L1 genes, the 5'UTR also contains an antisense promoter (ASP). This outward-oriented promoter drives transcription into adjacent genomic sequences, which potentially reduces transcript levels of nearby cellular genes due to interference with transcriptional elongation (Nigumann et al. 2002). This silencing effect of L1 ASP-derived transcripts may also contribute to the slightly lower expression levels of *KPL2* in ISTS-affected animals (II).
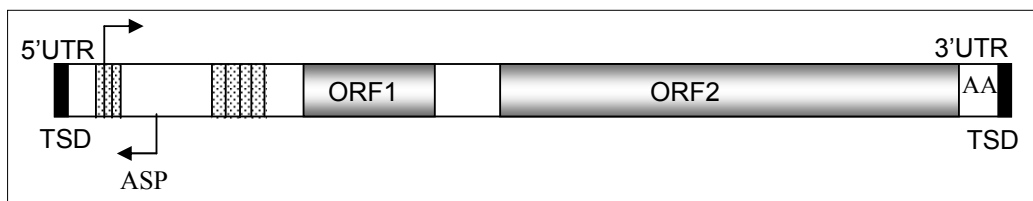

Figure 18. Structure of the L1-insertion within *KPL2* intron 30. TSD, target sequence duplication; ASP, antisense promoter; 5' and 3' UTR, untranslated regions; ORF1 and ORF2, open reading frames; AA, polyadenylation signal. The forward arrow indicates a bidirectional promoter and the dotted boxes highlight multiple repeat sequences. (Figure from III).

It has been shown that insertions within intron sequences may cause aberrant splicing events by disrupting regulatory regions (Mulhardt et al. 1994, Claverie-Martin et al. 2005). Sequence analysis of the target sequence of the L1 insertion showed that the intronic integration site is flanked by evolutionary conserved motifs (III), which may be involved in splicing regulation. The insertion may have occurred within a regulatory region, or it may relocate a regulatory motif, thus preventing its function (Lin et al. 1999,

Ganguly et al. 2003). However, the exact cause for aberrant splicing in ISTS-affected animals is not known.

6.1.4 DNA-test for gene assisted selection

Even though the carrier frequency was significantly reduced with MAS, the amount of ND cases prevented universal application of the test by pig breeders. Localization of the disease-causing mutation produced a 100% accurate DNA-test for gene assisted selection of the ISTS defect. The inaccuracies inherent to MAS could be overcome with a L1-based test and the disease status for all ND animals was able to be determined. Furthermore, parental samples were no longer required for reliable assessment of ISTS status. GAS enables the elimination of ISTS carriers from the Finnish Yorkshire pig population, but the decision to implement this test lies solely with pig breeders. Because of a putative positive correlation between ISTS and production traits, some ISTS carriers remain in the Finnish Yorkshire population, but the frequency of the defect is continually decreasing. The DNA-test was also used to elucidate the origin of the defect. Genotyping of different pig breeds showed that this defect appears to be exclusive to the Finnish Yorkshire (III), supporting the assumption of the recent origin of the ISTS in the Finnish Yorkshire population.

6.2 Expression pattern of KPL2

KPL2 is expressed in tissues containing cilia-like structures suggesting a role for this gene in ciliogenesis. *KPL2* expression is closely correlated with ciliated cell differentiation in cultures of primary tracheal epithelial cells (Ostrowski et al. 1999). Furthermore, the spatio-temporal expression pattern in seminiferous tubules at specific stages during murine spermatogenesis supports KPL2 as having a central role in the cilia/flagella formation. Analysis of KPL2 expression in model species provides valuable insights into the function of its products, since the KPL2 sequence is highly conserved across species. However, the expression of various *KPL2* transcript variants complicates the determination of KPL2 function. The long variant of *KPL2* appears to be testis specific indicating a unique role in spermiogenesis for this isoform. Various shorter transcript variants of *KPL2* also exist in the testis and other tissues (II, IV). In the human, two isoforms of *KPL2* have been identified, and several sequences with varying exon content from different tissues have been deposited in GenBank (Fig. 14).

6.2.1 Expression of KPL2 in porcine tissues

The long *KPL2* mRNA appeared to be mainly expressed in the testis, which accounts for the tissue specific symptoms of the truncated protein product. The expression of *KPL2* exon 30 was substantially lower in ISTS-affected boars relative to the expression in normal testis as a consequence of the altered splicing pattern. However, the loss of *KPL2* exon 30 was also seen in the trachea (II), but no respiratory dysfunction has been observed

in ISTS pigs. Microscopic examination of tracheal cilia also revealed no apparent effect on axonemal structure (unpublished results). The difference in the expression level of *KPL2* in the testis and trachea may indicate that the long *KPL2* variant has a more crucial role in sperm tail development than in cilia differentiation. This is supported by the fact that KPL2 protein appears to be localized in accessory structures of the sperm tail (IV). Furthermore, the expression of exon 30 was only slightly reduced in the trachea of ISTS-affected boars relative to the decrease in the testis (II). It is also possible that symptoms take longer to develop in the trachea, and would therefore not be detected in ISTS-affected boars because these animals are typically slaughtered at a young age once infertility has been diagnosed. However, the role of 3' end of *KPL2* seems to be more crucial for spermatogenesis than other vital functions.

The short form of *KPL2* (exons 7-8) was present in all examined tissues, except for the heart, highlighting a more general role for this *KPL2* variant (II). The short form is probably involved in cilia development as indicated in the rat (Ostrowski et al. 1999). Thus mutations in this part of *KPL2* would be more severe and affect various tissues. In rat tissues the expression pattern demonstrated a variant containing exons 20-22 of *Kpl2* (Ostrowski et al. 1999), which presumably resembles the expression pattern of pig exons 7-8. The expression of *KPL2* exons 7-8 in the pig was comparable with exons 20-22 in the rat with one exception. In the rat no expression of exons 20-22 was detected in hepatic tissue, but in the pig exons 7-8 were clearly expressed in the liver (II). These discrepancies may be due to different transcript variants or differences between species. The expression of *KPL2* exons 3-7 was also slightly reduced in ISTS-affected boars, possibly caused by mRNA degradation or via nonsense-mediated decay of incorrectly spliced long form transcripts or the silencing effect of L1 ASP. The expression pattern of exons 3-7 and 37-43 and the detection of two shorter KPL2 protein isoforms in western blot further support the occurrence of various *KPL2* transcript variants.

6.2.2 Expression of KPL2 in the murine testis

Expression of three different fragments (exons 3-7, 6-43 and 37-43) of *Kpl2* was investigated during the first wave of mouse spermatogenesis. All studied exons were expressed in the testis, which is consistent with the *KPL2* expression in pig tissues showing that the long *KPL2* variant 1 is testis-specific. A testis-specific fragment containing exons 6-43 first appeared simultaneously with late spermatocytes and round spermatids at PND 21. This may represent another testis specific transcript variant of *Kpl2* in addition to the long *Kpl2* variant 1. *Kpl2* exons 3-7 were first weakly expressed at PND 28. However, expression was significantly higher in adult testis indicating a role in sperm accessory structure formation. The *Kpl2* fragment containing exons 3-7 was also expressed in the lung, brain, kidney and liver, but exon 4 was depleted in these tissues. The expression of exons 3-7 can be assumed to represent the presence of the long

variant of *Kpl2*, which appears mutated in ISTS-affected boars. Interestingly, *Kpl2* exons 37-43 were expressed in the mouse testis throughout the first wave of spermatogenesis and also in the lung, brain, kidney and liver highlighting a more general role for this transcript variant in cilia development. Western blot showed the presence of a ~200 kDa KPL2 isoform at PND 21 which probably corresponds to exons 6-43. This isoform was also detected in the epididymis indicating that it is present in the sperm tail. However, the mRNA of the long *Kpl2* variant 1 was first detected in the testis at PND 28. The size difference of the long isoform 1 and the isoform containing exons 6-43 is probably too small to be clearly separated on an 8% acrylamide gel. The ~200 kDa KPL2 isoform detected in the epididymis appeared to be slightly shorter compared with the long KPL2 isoform in the testis at PND 42. These results infer that, at least in the mouse, the KPL2 isoform containing exons 6-43 is of functional importance in determining sperm tail structure and the long isoform 1 plays a role in sperm tail formation.

Expression of the 3'end (exon 43) of *Kpl2* has been shown to appear at PND 18 in microarray studies of the mouse testis (Schultz et al. 2003, Shima et al. 2004). This expression was also demonstrated in microarray experiments with pachytene spermatocytes and round spermatids (Namekawa et al. 2006) consistent with current findings of *Kpl2* expression profiles. In contrast to our results, previous studies did not detect any expression in SCs at PND 19. This discrepancy may be due to stage specific expression in SCs, specifically at crypt formation.

6.2.3   Spatio-temporal expression of KPL2 products

Kpl2 mRNA expression and localization were correlated with protein localization (Fig. 16). Detection of KPL2 protein in the sperm manchette at step 9 is consistent with the localization of the long form of *Kpl2* mRNA in spermatids. The localization in the midpiece of sperm tail confirms the presence of KPL2 in the sperm tail structure. Expression of a transcript variant of *Kpl2* in late spermatocytes is consistent with the expression of axonemal proteins (Horowitz et al. 2005, Fig. 19), although no protein product was detected in the axoneme of the sperm tail or in early spermatids (IV). The possible localization of KPL2 protein in late spermatocytes may arise from the *Kpl2* variant containing exons 6-43 in the mouse.

Histological results imply that a shorter form of KPL2 may be involved in the Golgi complex, since KPL2 was also present in the Golgi of ISTS-affected spermatids (IV). KPL2 staining was also detected in spermatid bundles of the mouse and pig indicating a role for KPL2 in SC/germ cell junctions. KPL2 staining was detected in SC cytoplasm prior to bundle formation, suggesting that this possible KPL2 isoform originates from SC expression. Interestingly, a reduction of the KPL2 protein in SC cytoplasm of ISTS boars was detected in cryosections, while KPL2 staining was present in spermatid bundles of ISTS squash preparations (unpublished data). This difference in KPL2 staining pattern

in SC cytoplasm of WT and ISTS boars may be due to secondary effects of the mutation, since SC gene expression has been shown to be affected by germ cells (O'Shaughnessy et al. 2008, Vidal et al. 2001). The organization of germ cells in the seminiferous tubules of ISTS boars appeared to be disrupted suggesting that KPL2 may affect the connection between SCs and germ cells (unpublished data). However, the possible staining of SCs appeared prior to bundle formation complicating the detection of KPL2 mRNA or protein in purified SCs. Further studies are required to confirm KPL2 localization in SCs.

It is possible that the function of KPL2 may differ between species despite the highly conserved nature of the KPL2 protein sequence. Thus far, the appearance of short isoforms of KPL2 in the mouse and pig has not been confirmed and data from expression studies indicate at least some differences between species. However, the expression of the long isoform 1 of KPL2 appears to be testis specific in both species. This isoform 1 is expressed simultaneously with ODF and FS genes (Horowitz et al. 2005, Fig. 19) implicating the functional importance in the formation of sperm tail accessory structures. Furthermore, expression pattern of exons 37-43 suggests a more general role of KPL2 in spermatogenesis.
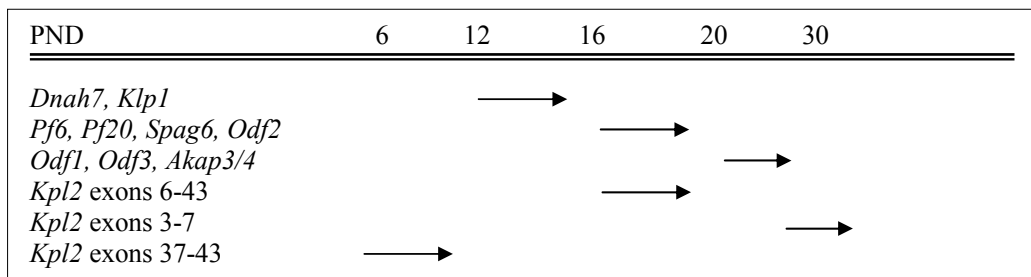
Figure 19. Expression pattern of genes involved in the formation of axonemal and accessory structures in the mouse sperm flagella (Horowitz et al. 2005) compared with the expression of different *Kpl2* fragments. The timeframe of spermatogenesis is indicated in PND. Genes involved in axoneme development are first expressed at PND 16 and genes associated with sperm accessory structures at PND 20. *Kpl2* exons 6-43 are expressed simultaneously with axonemal genes and the long form of *Kpl2* with accessory structure genes. In addition, some gene product of *Kpl2* exons 37-43 was apparent on PND 7.

6.3   Implication of KPL2 and its function

Kpl2 expression correlates with ciliated cell differentiation and dynein expression *in vitro* (Ostrowski et al. 1999). This suggests that KPL2 may be involved in axoneme development. However, in ISTS-affected pigs the lack of the long form of KPL2 only affects the structure and function of the sperm tail, indicating a specific functional importance of at least one isoform of KPL2 in the testis. On the other hand, studies of *KPL2* gene expression in the rat, pig and mouse further confirm the association between KPL2 and ciliated cells and implicate at least two separate functions of KPL2 in cilia/flagella development.

6.3.1　Domain structure and conservation of KPL2

The KPL2 protein sequence was shown to be highly conserved among mammalian species and several functional domains were identified. The presence of a DUF1042 domain in the N-terminus (Fig. 20) classifies KPL2 together with other proteins implicated in flagella function including human SPATA4 protein (spermatogenesis associate 4, NP_653245), mouse sperm flagella protein SPEF1 (AY860964) and CPC1 (central pair complex 1, AAT40991) of the unicellular organism *Chlamydomonas reinhardtii*. KPL2 is also referred to as SPEF2 belonging to the SPEF protein family with SPEF1 (Chan et al. 2005). Furthermore, KPL2 and CPC1 share greater than 40% similarity over most of the length of these proteins and both harbour several common functional domains (DUF1042, ADK and EF-hands, Fig. 20) suggesting that they serve similar functions. Furthermore, four α-helical coiled-coils were predicted in CPC1 suggesting that CPC1 functions as an extended structural protein. These amino-terminal α-helical coiled-coil domains and their
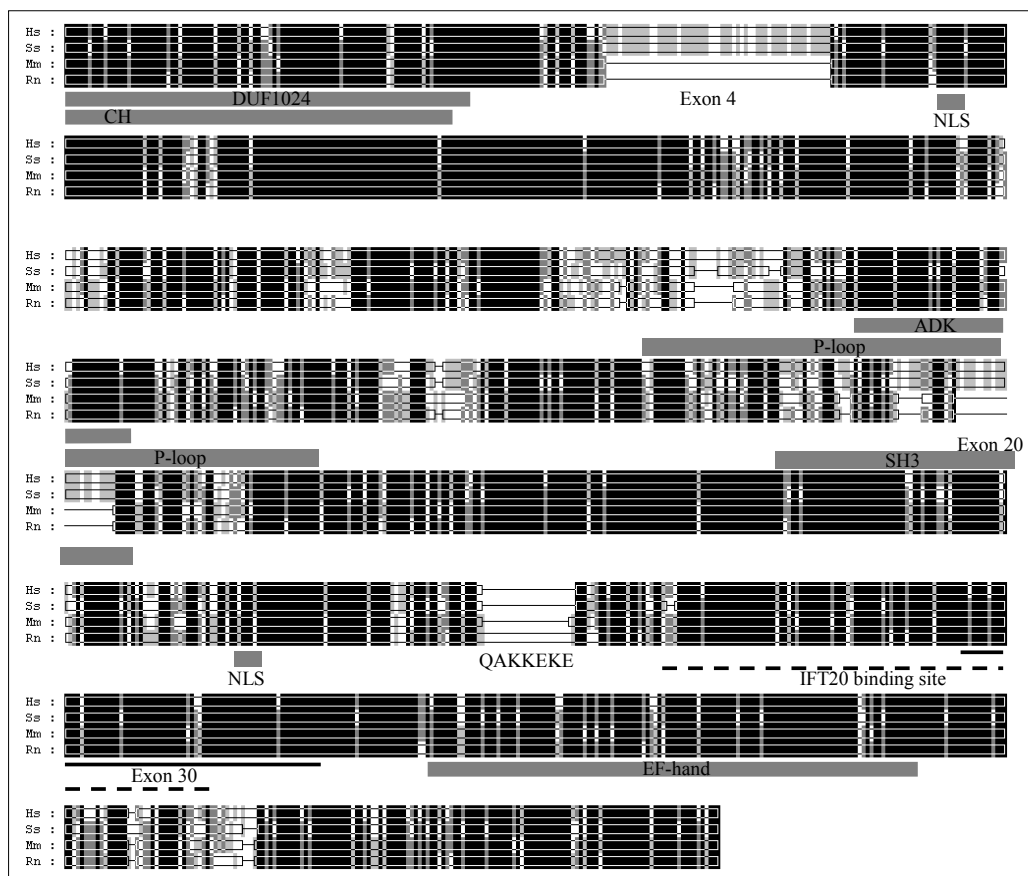
Figure 20. Alignment of KPL2 protein sequences in the human (Hs, NP_079143), pig (Ss, NP_001038026), mouse (Mm, Q8C9J3) and rat (Rn, NP_072142). Identical residues are shaded in black and conserved replacements in grey. Missing amino acids in sequences (exons 4, 20 and QAKKEKE-repeat) are highlighted. Based on our results exon 4 is present in the testis variant of murine *Kpl2*. Exon 30 is indicated by a solid line, predicted motifs with a grey bar and a possible binding site for IFT20 by dashed line.

linker domains have been predicted to be similar to KPL2 (Zhang and Mitchell. 2004) and a Smart search determined two coiled coils for KPL2 in the pig (amino-terminal).

Mutations in *cpc1* disrupt the assembly of the central pair microtubule-associated complex and alter flagellar beat frequency (Zhang and Mitchell. 2004). Adenylate kinases can maintain local ATP concentrations (Nakamura et al. 1999) and in *Chlamydomonas* flagella a lack of CPC1 results in the inability to maintain a sufficiently high ATP concentration within the axoneme. Since motility can be restored with additional ATP and ADP, these axonemes must contain other adenylate kinases (Zhang and Mitchell. 2004). CPC1 co-sediments with five additional proteins, which fail to assemble in axonemes deficient in CPC1. These co-sedimented proteins may therefore contribute to the reduction of local ATP. The CPC1 complex includes C_160167 (C. reinhardtii genome database v 2.0) with ADK and five guanylate-domains, mostly alpha helical C_340095, heat-shock protein HSP70A (C_1340012) and a glycolytic enzyme enolase (C_160138, Mitchell et al. 2005). In mammals, the sperm specific form of enolase has been localized to the sperm tail in a nucleotide-dependent association with microtubules (Edwards and Grootegoed. 1983, Gitlits et al. 2000). In *Chlamydomonas* flagella the CPC1 complex may be important for anchoring enolase in the flagellar compartment, although some enolase remains in the cytoplasm. The reduced intraflagellar ATP concentrations may result from the lack of enolase in the CPC1 mutant. In trypanosomes, >80% reduction in flagellar AK activity has no detectable effect on flagellar beat activity (Pullen et al. 2004). The diffusion of ATP from the cytoplasm probably maintains motility in the absence of the CPC1 complex. ATP is also essential for IFT and protein kinases, even though these functions are not affected in known CPC1 mutants (Mitchell et al. 2005). Given the similarity between KPL2 and CPC1, a reduction in ATP levels might affect sperm tail formation in ISTS-affected pigs in addition to the effects on sperm tail structure.

CPC1 mutants also lack HSP70A, a component located to the cell body and flagella of *Chlamydomonas*, which may assist with the folding and delivery of flagellar proteins (Shapiro et al. 2005). Localization to the CPC1 complex also suggests that HSP70A could act as a conformational switch for the central pair regulation of motility (Mitchell et al. 2005). The CPC1 complex has also been shown to interact with hydin, while RNA interference of hydin results in short flagella (Lechtreck and Witman. 2007).

The results from CPC1 provide important information about the possible function of KPL2, but establishing exact protein interactions of KPL2 require additional experiments. The *KPL2* mutation produces a complex and more severe phenotype than the lack of CPC1 with fully disrupted central pair microtubules, as well as accessory structure defects. These observations suggest different or additional roles of KPL2 in the assembly of the sperm tail. However, it should be noted that the ISTS mutation may have additional effects than those on the long isoform of the KPL2 protein. It appears that the

long isoform also hinders the normal removal of short KPL2 isoforms from the maturing ISTS sperm tail (IV). Additionally, the L1 insertion may affect expression of adjacent genes through the ASP promoter (Nigumann et al. 2002). Since no effect on tracheal cilia was observed in ISTS-affected animals, the function of the KPL2 isoform 1 in axonemal structures appears to be dependent on sperm tail accessory structures. The C-terminal part of KPL2 protein sequence (1577-1812aa in porcine sequence) is not present in the CPC1 sequence, which may indicate that this part of the protein is only a prerequisite when KPL2 is involved in sperm tail development. Other parts of the protein may also be involved in the testis specific function, for example exon 4.

In addition to the possible link between KPL2 and decreases in ATP levels, a calcium-binding EF-hand motif infers an additional role of KPL2 in calcium signaling. Interactions of KPL2 with the cytoskeleton are supported by the presence of a calponin homology (CH) domain in the N-terminus (Fig. 20). This domain is found in cytoskeletal and signal transduction proteins pointing towards potential actin binding activity. However, all CH domains are not involved in actin binding; hence the actin binding capacity of KPL2 is not evident. An SH3 interacting domain indicates an involvement in signal transduction related to cytoskeletal organisation. Interestingly, the SH3 domain has been identified in IFT52 (OSM-6, Collet et al. 1998) and IFT proteins have been shown to be rich in interaction domains (Cole. 2003) supporting the possible role of KPL2 in IFT. It is also possible that KPL2 may perform at least part of its function in the nucleus, since two potential bipartite nuclear localization signals were predicted (II).

6.3.2 The role of KPL2 in sperm tail development

Since CPC1 has been shown to interact with the axonemal central pair complex (Zhang and Mitchell. 2004), the homology of KPL2 with CPC1 suggests similar functions for these proteins. However, late localization of KPL2 to the sperm tail during spermatogenesis in the mouse is not consistent with a role of KPL2 as a structural protein in the axoneme, but does confirm the assumption that KPL2 is involved in sperm tail formation. Our protein localization results represent KPL2 isoforms containing exon 43. In addition, shorter forms of KPL2 may also exist and interact with the axoneme. Localization of KPL2 protein products in the manchette, basal body and midpiece of elongating spermatids (IV) suggests that KPL2 may operate in a co-ordinated manner with IMT/IFT proteins. The high amount of KPL2 protein in the residual body of elongated spermatids also highlights a temporal role in sperm tail development. Even though CPC1 has not been shown to be involved in IFT, a possible interacting partner of CPC1, HSP70A, may assist in the folding and delivery of flagellar proteins (Shapiro et al. 2005). Furthermore, in ISTS-affected boars all sperm tail structures were disorganized indicating that a mutation in *KPL2* disrupts the whole sperm tail assembly. Finally, we detected a possible interaction between KPL2 and an identified IFT protein, IFT20.

Previous studies have indicated that the manchette may have an important role in IMT and IFT by sorting the structural proteins to the centrosome and the developing sperm tail (Kierszenbaum. 2002, Kierszenbaum. 2001, Rivkin et al. 1997, Tres and Kierszenbaum. 1996). Our localization of IFT20 protein in the manchette supports the supposed role of manchette in IFT (IV). The manchette is a microtubular structure forming after the axoneme has been assembled. It is central to the shaping and condensation of the sperm nucleus and also for the assembly of the mammalian sperm tail (Kierszenbaum. 2002). Both IMT and IFT involve molecular motors (primarily kinesins and dyneins) mobilizing a multicomplex protein rafts to which cargo proteins or vesicles are linked. Manchette proteins are relocated to centrosomes and the sperm tail upon manchette disassembly, soon after the elongation and condensation of the spermatid nucleus is near completion (Kierszenbaum. 2002). KPL2 protein relocates from the manchette first to the basal body and neck region at step 13-14 during manchette disassembly (IV, Fig. 21). Structural proteins have also been located in the manchette prior to transportation in the sperm tail. For example, SPAG4 localizes to the manchette and microtubules in step 10 spermatids and at later stages of spermatid development with ODF1 (Shao et al. 1999). These observations may infer a structural role of KPL2 in the sperm tail.

IFT proteins are mainly present in the base of the flagella with only small amounts in the flagella themselves (Follit et al. 2006). A possible involvement of KPL2 with the IFT system was detected by an interaction with IFT20. Co-localization of IFT20 and KPL2 showed that these proteins may interact in the manchette and basal body of step 9-14 spermatids (IV, Fig. 21). However, there was no evidence in ISTS-affected boars to support that this interaction is the cause for the sperm tail malformation. Interplay between KPL2 and IFT20 was also observed in the brain indicating a general role for this interaction in cilia development. Another possible site for the interaction between KPL2 and IFT20 was detected in the Golgi complex. Previously, IFT20 has been located in the basal body, cilia and the Golgi complex of ciliary cell lines (Follit et al. 2006). In the present study, IFT20 was located in the Golgi complex of murine late spermatocytes and spermatids (IV). KPL2 was also detected in the Golgi of murine late spermatocytes and porcine spermatids (Fig. 17). In the pig, co-localization with the Golgi marker HPA indicated that KPL2 is mainly present in the trans-Golgi compartment. This suggests a role in the final packaging and delivery of proteins. It has been proposed that the possible role of IFT20 in the Golgi complex is to mark vesicles containing proteins destined for the ciliary membrane (Follit et al. 2006). KPL2 may serve a similar function, or it may simply be stored and/or modified in the Golgi complex and transported to the cilia by the interaction with IFT20. However, localization of KPL2 in the Golgi complex requires further studies.
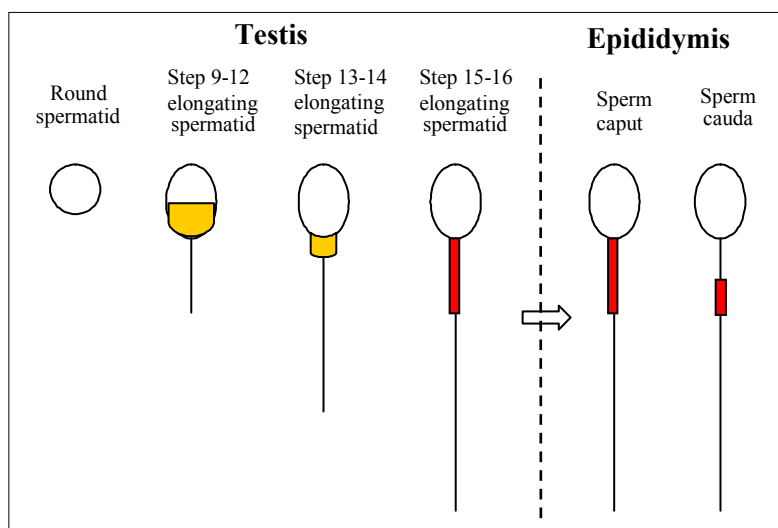
Figure 21. Localization of KPL2 and IFT20 proteins during sperm tail development and maturation. KPL2 and IFT20 (co-localization indicated in yellow) are first detected in the sperm manchette in step 9 elongating spermatids and move to the basal body at step 13. Around steps 13-14, KPL2 further relocates to the neck region of the sperm tail and at step 15 (indicated in red) along the midpiece. In epididymal sperm, KPL2 is first present in the midpiece of the sperm tail and concentrates in the distal part of the midpiece during sperm maturation.

IFT motorprotein dynein has been localized to spermatid manchettes, SCs (Hall et al. 1992, Yoshida et al. 1994, Yoshida et al. 1992) and ectoplasmic specializations (Hall et al. 1992), while another motorprotein kinesin has been located in the sperm tail midpiece (Henson et al. 1997), the SC-Golgi network and manchette (Johnson et al. 1996) in the rat testis. Thus, IFT particles may play additional roles beyond the classical IFT system. Identification of possible KPL2 localizations in SCs, ectoplasmic specializations and the Golgi complex may reflect an association of KPL2 with these structures. A shorter form of KPL2 including exons 6-43 was expressed simultaneously with axonemal genes (IV), suggesting that this part of KPL2 also has a role in axoneme formation in the sperm tail. The likely localization of this shorter form of KPL2 protein was detected in the Golgi complex in late primary spermatocytes (unpublished data) or in SCs and spermatid bundles (IV). KPL2 localization in the Golgi complex could affect the delivery of axonemal proteins, resulting in axonemal defects. However, Golgi staining of KPL2 was not affected in ISTS boars (IV). Although no KPL2 staining was detected in the axoneme, it may still associate with axonemal structures owing to the lack of specificity in the immunohistochemical assays.

KPL2 protein first appeared in the manchette of elongating spermatids at step 9 suggesting that this localization was associated with the long form of KPL2 (IV). KPL2 may have a role in the delivery of cilia/flagella proteins and/or it may function as a structural protein in cilia/flagella. However, a mutation affecting the long form of KPL2 affects

all structures of the sperm tail demonstrating diverse effects in sperm tail formation. The mutated form of KPL2 in pigs does not affect axoneme structure in other cilia with the implication that another KPL2 isoform functions in general axoneme development. Based on these data it would not necessarily be expected that the testis specific isoform is present in the axoneme, but the effect seen in the sperm tail is a consequence of a malfunction in the delivery of flagellar proteins and/or assembly of accessory structures of the sperm tail. It has been shown that defects of sperm accessory structures affect the axonemal structure, but the exact mechanism is not known (Rawe et al. 2001). However, it appears unlikely that KPL2 localization in the midpiece of sperm tail simultaneously with mitochondrial sheath formation causes all the malformations in ISTS-affected sperm, and as such a role of KPL2 in protein delivery seems probable.

Our findings have elucidated several possible roles of KPL2 in spermatogenesis, although establishing the exact functions of KPL2 requires further investigation. Identification of KPL2 interacting partners in the future will provide further insights into the functions of KPL2 in the testis. The presence of different transcript variants of *KPL2* in various tissues indicates a wider role for this gene in cilia development and possibly some other, as yet, unidentified functions. Future studies of the function of KPL2 in other ciliated cells are required to elucidate the role of various KPL2 isoforms.

7.   CONCLUSIONS

Male infertility is becoming an increasing problem, partly because of environmental factors, but many defects in the sperm development arise from genetic causes. Despite efforts to identify genes and their functions in spermatogenesis, little is known about the underlying causes of male infertility. Considerable research has been devoted to the *Chlamydomonas* model to understand axonemal function in cilia and flagella. Even though studies in *Chlamydomonas* have provided an insight into cilia development, mammalian models are needed to establish the genetic causes for spermatozoa dysfunction. The ISTS mutation in the Finnish Yorkshire pig offers a unique opportunity to study male infertility in an animal model. Since the defect incurred substantial costs to pig breeding in Finland, we developed a genetic test for selection against the defect. Furthermore, the ISTS defect in pigs affecting sperm tail structure and motility allows a detailed investigation of an infertility associated gene, which may also be the causative mechanism for some cases of human male infertility.

Elucidation of KPL2 protein functions enables a better understanding of events integral to the formation and motility of spermatozoa. The ISTS defect is caused by an active L1 insertion within *KPL2* intron 30, resulting in aberrant splicing of exon 30. Although several transcript variants of *KPL2* exist in various tissues, available evidence suggests that this insertion only affects the testis specific long variant of *KPL2*. This long isoform appears to be involved in the formation of flagellar accessory structures, since a lack of this protein product in the ISTS defect only alters sperm tail development. However, the axonemal structure of flagella was also disorganized in ISTS-affected boars with the implication that it is affected by the mutated *KPL2* either during protein delivery or mediated via accessory structures. In the mouse, the localization of KPL2 protein in the spermatid manchette and basal body indicates a role in flagellar protein delivery through IFT or IMT. This was further supported by the interplay and co-localization with an identified IFT protein IFT20. KPL2 also occurs simultaneously with mitochondrial sheath formation in the murine sperm tail, which suggests an additional structural function in the sperm tail midpiece. However, tissue and phase specific variants of KPL2 appear to be present in the testis and other tissues, thus KPL2 probably has other, as yet, undefined roles.

8. ACKNOWLEDGEMENTS

9.   REFERENCES

Adams GM, Huang B, Piperno G, Luck DJ. Central-pair microtubular complex of Chlamydomonas flagella: polypeptide composition as revealed by analysis of mutants. J.Cell Biol. 1981 Oct;91(1):69-76.

Afzelius BA. Cilia-related diseases. J.Pathol. 2004 Nov;204(4):470-7.

Afzelius BA. A human syndrome caused by immotile cilia. Science 1976 Jul 23;193(4250):317-9.

Ahmed NT, Mitchell DR. ODA16p, a Chlamydomonas flagellar protein needed for dynein assembly. Mol.Biol.Cell 2005 Oct;16(10):5004-12.

Anderson SI, Lopez-Corrales NL, Gorick B, Archibald AL. A large-fragment porcine genomic library resource in a BAC vector. Mamm.Genome 2000 Sep;11(9):811-4.

Andersson M, Peltoniemi O, Makinen A, Sukura A, Rodriguez-Martinez H. The Hereditary 'Short Tail' Sperm Defect - A New Reproductive Problem in Yorkshire Boars. Reproduction in Domestic Animals 2000;35(2):59.

Ansley SJ, Badano JL, Blacque OE, Hill J, Hoskins BE, Leitch CC, et al. Basal body dysfunction is a likely cause of pleiotropic Bardet-Biedl syndrome. Nature 2003 Oct 9;425(6958):628-33.

Aravin AA, Hannon GJ, Brennecke J. The Piwi-piRNA pathway provides an adaptive defense in the transposon arms race. Science 2007 Nov 2;318(5851):761-4.

Babushok DV, Kazazian HH,Jr. Progress in understanding the biology of the human mutagen LINE-1. Hum.Mutat. 2007 Jun;28(6):527-39.

Baccetti B, Burrini AG, Capitani S, Collodel G, Moretti E, Piomboni P, et al. Notulae seminologicae. 2. The 'short tail' and 'stump' defect in human spermatozoa. Andrologia 1993 Nov-Dec;25(6):331-5.

Baccetti B, Capitani S, Collodel G, Di Cairano G, Gambera L, Moretti E, et al. Genetic sperm defects and consanguinity. Hum.Reprod. 2001 Jul;16(7):1365-71.

Baccetti B, Collodel G, Crisa D, Moretti E, Piomboni P. Notulae seminologicae. 8.Ultrastructural sperm defects in two men, carriers of autosomal inversion. Andrologia 1997 Sep-Oct;29(5):277-82.

Baccetti B, Collodel G, Estenoz M, Manca D, Moretti E, Piomboni P. Gene deletions in an infertile man with sperm fibrous sheath dysplasia. Hum.Reprod. 2005a Oct;20(10):2790-4.

Baccetti B, Collodel G, Gambera L, Moretti E, Serafini F, Piomboni P. Fluorescence in situ hybridization and molecular studies in infertile men with dysplasia of the fibrous sheath. Fertil.Steril. 2005b Jul;84(1):123-9.

Barthelemy C, Tharanne MJ, Lebos C, Lecomte P, Lansac J. Tail stump spermatozoa: morphogenesis of the defect. An ultrastructural study of sperm and testicular biopsy. Andrologia 1990 Sep-Oct;22(5):417-25.

Bartoloni L, Blouin JL, Pan Y, Gehrig C, Maiti AK, Scamuffa N, et al. Mutations in the DNAH11 (axonemal heavy chain dynein type 11) gene cause one form of situs inversus totalis and most likely primary ciliary dyskinesia. Proc.Natl.Acad.Sci.U.S.A. 2002 Aug 6;99(16):10282-6.

Bellve AR, Cavicchia JC, Millette CF, O'Brien DA, Bhatnagar YM, Dym M. Spermatogenic cells of the prepuberal mouse. Isolation and morphological characterization. J.Cell Biol. 1977 Jul;74(1):68-85.

Blendy JA, Kaestner KH, Weinbauer GF, Nieschlag E, Schutz G. Severe impairment of spermatogenesis in mice lacking the CREM gene. Nature 1996 Mar 14;380(6570):162-5.

Blom E. A sterilizing tail stump sperm defect in a Holstein-Friesian bull. Nord.Vet.Med. 1976 Jun;28(6):295-8.

Boer PH, Adra CN, Lau YF, McBurney MW. The testis-specific phosphoglycerate kinase gene pgk-2 is a recruited retroposon. Mol.Cell.Biol. 1987 Sep;7(9):3107-12.

Bouchard MJ, Dong Y, McDermott BM,Jr, Lam DH, Brown KR, Shelanski M, et al. Defects in nuclear and cytoskeletal morphology and mitochondrial localization in spermatozoa of mice lacking nectin-2, a component of cell-cell adherens junctions. Mol.Cell.Biol. 2000 Apr;20(8):2865-73.

Boyle CA, Khoury MJ, Katz DF, Annest JL, Kresnow MJ, DeStefano F, et al. The relation of computer-based measures of sperm morphology and motility to male infertility. Epidemiology 1992 May;3(3):239-46.

Brohmann H, Pinnecke S, Hoyer-Fender S. Identification and characterization of new cDNAs encoding outer dense fiber proteins of rat sperm. J.Biol.Chem. 1997 Apr 11;272(15):10327-32.

Brown PR, Miki K, Harper DB, Eddy EM. A-kinase anchoring protein 4 binding proteins in the fibrous sheath of the sperm flagellum. Biol.Reprod. 2003 Jun;68(6):2241-8.

Budny B, Chen W, Omran H, Fliegauf M, Tzschach A, Wisniewska M, et al. A novel X-linked recessive mental retardation syndrome comprising macrocephaly and ciliary dysfunction is allelic to oral-facial-digital type I syndrome. Hum.Genet. 2006 Sep;120(2):171-8.

Burgos C, Maldonado C, Gerez de Burgos NM, Aoki A, Blanco A. Intracellular localization of the testicular and sperm-specific lactate dehydrogenase isozyme C4 in mice. Biol.Reprod. 1995 Jul;53(1):84-92.

Burmester S, Hoyer-Fender S. Transcription and translation of the outer dense fiber gene (Odf1) during spermiogenesis in the rat. A study by in situ analyses and polysome fractionation. Mol. Reprod.Dev. 1996 Sep;45(1):10-20.

Cao W, Gerton GL, Moss SB. Proteomic profiling of accessory structures from the mouse sperm flagellum. Mol.Cell.Proteomics 2006a May;5(5):801-10.

Cao W, Haig-Ladewig L, Gerton GL, Moss SB. Adenylate kinases 1 and 2 are part of the accessory structures in the mouse sperm flagellum. Biol. Reprod. 2006b Oct;75(4):492-500.

Catalano RD, Hillhouse EW, Vlad M. Developmental expression and characterization of FS39, a testis complementary DNA encoding an intermediate filament-related protein of the sperm fibrous sheath. Biol.Reprod. 2001 Jul;65(1):277-87.

Chan SW, Fowler KJ, Choo KH, Kalitsis P. Spef1, a conserved novel testis protein found in mouse sperm flagella. Gene 2005 Jul 4;353(2):189-99.

Chemes HE. Phenotypes of sperm pathology: genetic and acquired forms in infertile men. J.Androl. 2000 Nov-Dec;21(6):799-808.

Chemes HE, Morero JL, Lavieri JC. Extreme asthenozoospermia and chronic respiratory disease: a new variant of the immotile cilia syndrome. Int.J.Androl. 1990 Jun;13(3):216-22.

Chemes HE, Olmedo SB, Carrere C, Oses R, Carizza C, Leisner M, et al. Ultrastructural pathology of the sperm flagellum: association between flagellar pathology and fertility prognosis in severely asthenozoospermic men. Hum.Reprod. 1998 Sep;13(9):2521-6.

Chodhari R, Mitchison HM, Meeks M. Cilia, primary ciliary dyskinesia and molecular genetics. Paediatr.Respir.Rev. 2004 Mar;5(1):69-76.

Claverie-Martin F, Flores C, Anton-Gamero M, Gonzalez-Acosta H, Garcia-Nieto V. The Alu insertion in the CLCN5 gene of a patient with Dent's disease leads to exon 11 skipping. J.Hum. Genet. 2005;50(7):370-4.

Clermont Y, Oko R, Hermo L. Immunocytochemical localization of proteins utilized in the formation of outer dense fibers and fibrous sheath in rat spermatids: an electron microscope study. Anat. Rec. 1990 Aug;227(4):447-57.

Cole DG. The intraflagellar transport machinery of Chlamydomonas reinhardtii. Traffic 2003 Jul;4(7):435-42.

Collet J, Spike CA, Lundquist EA, Shaw JE, Herman RK. Analysis of osm-6, a gene that affects sensory cilium structure and sensory neuron function in Caenorhabditis elegans. Genetics 1998 Jan;148(1):187-200.

Dacheux JL, Gatti JL, Dacheux F. Contribution of epididymal secretory proteins for spermatozoa maturation. Microsc.Res.Tech. 2003 May 1;61(1):7-17.

Deane JA, Ricardo SD. Polycystic kidney disease and the renal cilium. Nephrology (Carlton) 2007 Dec;12(6):559-64.

Deng W, Lin H. Miwi, a Murine Homolog of Piwi, Encodes a Cytoplasmic Protein Essential for Spermatogenesis. Dev.Cell. 2002 Jun;2(6):819-30.

Duriez B, Duquesnoy P, Escudier E, Bridoux AM, Escalier D, Rayet I, et al. A common variant in combination with a nonsense mutation in a member of the thioredoxin family causes primary ciliary dyskinesia. Proc.Natl.Acad.Sci.U.S.A. 2007 Feb 27;104(9):3336-41.

Eddy EM, Toshimori K, O'Brien DA. Fibrous sheath of mammalian spermatozoa. Microsc.Res. Tech. 2003 May 1;61(1):103-15.

Edwards YH, Grootegoed JA. A sperm-specific enolase. J.Reprod.Fertil. 1983 Jul;68(2):305-10.

Escalier D. Knockout mouse models of sperm flagellum anomalies. Hum.Reprod.Update 2006 Jul-Aug;12(4):449-61.

Fawcett DW. The anatomy of the spermatozoon after 300 years. Kaibogaku Zasshi 1975 Dec;50(6):326-7.

Fawcett DW, Phillips DM. The fine structure and development of the neck region of the mammalian spermatozoon. Anat.Rec. 1969 Oct;165(2):153-64.

Feiden S, Wolfrum U, Wegener G, Kamp G. Expression and compartmentalisation of the glycolytic enzymes GAPDH and pyruvate kinase in boar spermatogenesis. Reprod.Fertil.Dev. 2008;20(6):713-23.

Fliegauf M, Benzing T, Omran H. When cilia go bad: cilia defects and ciliopathies. Nat.Rev.Mol. Cell Biol. 2007 Nov;8(11):880-93.

Follit JA, Tuft RA, Fogarty KE, Pazour GJ. The intraflagellar transport protein IFT20 is associated with the Golgi complex and is required for cilia assembly. Mol.Biol.Cell 2006 Sep;17(9):3781-92.

Ganguly A, Dunbar T, Chen P, Godmilow L, Ganguly T. Exon skipping caused by an intronic insertion of a young Alu Yb9 element leads to severe hemophilia A. Hum.Genet. 2003 Sep;113(4):348-52.

Gietz RD, Woods RA. Transformation of yeast by lithium acetate/single-stranded carrier DNA/ polyethylene glycol method. Methods Enzymol. 2002;350:87-96.

Gitlits VM, Toh BH, Loveland KL, Sentry JW. The glycolytic enzyme enolase is present in sperm tail and displays nucleotide-dependent association with microtubules. Eur.J.Cell Biol. 2000 Feb;79(2):104-11.

Griswold MD. The central role of Sertoli cells in spermatogenesis. Semin.Cell Dev.Biol. 1998 Aug;9(4):411-6.

Hackstein JH, Hochstenbach R, Pearson PL. Towards an understanding of the genetics of human male infertility: lessons from flies. Trends Genet. 2000 Dec;16(12):565-72.

Hall ES, Eveleth J, Jiang C, Redenbach DM, Boekelheide K. Distribution of the microtubule-dependent motors cytoplasmic dynein and kinesin in rat testis. Biol.Reprod. 1992 May;46(5):817-28.

Han JS, Boeke JD. LINE-1 retrotransposons: modulators of quantity and quality of mammalian gene expression? Bioessays 2005 Aug;27(8):775-84.

Heckert LL, Griswold MD. The expression of the follicle-stimulating hormone receptor in spermatogenesis. Recent Prog.Horm.Res. 2002;57:129-48.

Heller CG, Clermont Y. Spermatogenesis in man: an estimate of its duration. Science 1963 Apr 12;140:184-6.

Henson JH, Cole DG, Roesener CD, Capuano S, Mendola RJ, Scholey JM. The heterotrimeric motor protein kinesin-II localizes to the midpiece and flagellum of sea urchin and sand dollar sperm. Cell Motil.Cytoskeleton 1997;38(1):29-37.

Hoffman CS, Winston F. A ten-minute DNA preparation from yeast efficiently releases autonomous plasmids for transformation of Escherichia coli. Gene 1987;57(2-3):267-72.

Hogeveen KN, Sassone-Corsi P. Regulation of gene expression in post-meiotic male germ cells: CREM-signalling pathways and male fertility. Hum.Fertil.(Camb) 2006 Jun;9(2):73-9.

Holdcraft RW, Braun RE. Hormonal regulation of spermatogenesis. Int.J.Androl. 2004 Dec;27(6):335-42.

Horowitz E, Zhang Z, Jones BH, Moss SB, Ho C, Wood JR, et al. Patterns of expression of sperm flagellar genes: early expression of genes encoding axonemal proteins during the spermatogenic cycle and shared features of promoters of genes encoding central apparatus proteins. Mol.Hum. Reprod. 2005 Apr;11(4):307-17.

Hoyer-Fender S, Burfeind P, Hameister H. Sequence of mouse Odf1 cDNA and its chromosomal localization: extension of the linkage group between human chromosome 8 and mouse chromosome 15. Cytogenet.Cell Genet. 1995;70(3-4):200-4.

Ihara M, Kinoshita A, Yamada S, Tanaka H, Tanigaki A, Kitano A, et al. Cortical organization by the septin cytoskeleton is essential for structural and mechanical integrity of mammalian spermatozoa. Dev.Cell. 2005 Mar;8(3):343-52.

Inaba K. Molecular architecture of the sperm flagella: molecules for motility and signaling. Zoolog Sci. 2003 Sep;20(9):1043-56.

Insinna C, Besharse JC. Intraflagellar transport and the sensory outer segment of vertebrate photoreceptors. Dev.Dyn. 2008 Aug;237(8):1982-92.

Irons MJ, Clermont Y. Formation of the outer dense fibers during spermiogenesis in the rat. Anat.Rec. 1982 Apr;202(4):463-71.

Johnson KJ, Hall ES, Boekelheide K. Kinesin localizes to the trans-Golgi network regardless of microtubule organization. Eur.J.Cell Biol. 1996 Mar;69(3):276-87.

Katsanis N, Lupski JR, Beales PL. Exploring the molecular basis of Bardet-Biedl syndrome. Hum. Mol.Genet. 2001 Oct 1;10(20):2293-9.

Kierszenbaum AL. Intramanchette transport (IMT): managing the making of the spermatid head, centrosome, and tail. Mol.Reprod.Dev. 2002 Sep;63(1):1-4.

Kierszenbaum AL. Spermatid manchette: plugging proteins to zero into the sperm tail. Mol.Reprod. Dev. 2001 Aug;59(4):347-9.

King SM. The dynein microtubule motor. Biochim. Biophys.Acta 2000 Mar 17;1496(1):60-75.

Kissel H, Georgescu MM, Larisch S, Manova K, Hunnicutt GR, Steller H. The Sept4 septin locus is required for sperm terminal differentiation in mice. Dev.Cell. 2005 Mar;8(3):353-64.

Klattenhoff C, Theurkauf W. Biogenesis and germline functions of piRNAs. Development 2008 Jan;135(1):3-9.

Kolettis PN. Evaluation of the subfertile man. Am.Fam.Physician 2003 May 15;67(10):2165-72.

Kotaja N, Lin H, Parvinen M, Sassone-Corsi P. Interplay of PIWI/Argonaute protein MIWI and kinesin KIF17b in chromatoid bodies of male germ cells. J.Cell.Sci. 2006 Jul 1;119(Pt 13):2819-25.

Kotaja N, Sassone-Corsi P. The chromatoid body: a germ-cell-specific RNA-processing centre. Nat. Rev.Mol.Cell Biol. 2007 Jan;8(1):85-90.

Kruglyak L, Daly MJ, Reeve-Daly MP, Lander ES. Parametric and nonparametric linkage analysis: a unified multipoint approach. Am.J.Hum.Genet. 1996 Jun;58(6):1347-63.

Kuramochi-Miyagawa S, Kimura T, Ijiri TW, Isobe T, Asada N, Fujita Y, et al. Mili, a mammalian member of piwi family gene, is essential for spermatogenesis. Development 2004 Feb;131(4):839-49.

Lander ES, Botstein D. Homozygosity mapping: a way to map human recessive traits with the DNA of inbred children. Science 1987 Jun 19;236(4808):1567-70.

Lechtreck KF, Witman GB. Chlamydomonas reinhardtii hydin is a central pair protein required for flagellar motility. J.Cell Biol. 2007 Feb 12;176(4):473-82.

Lehman JM, Laag E, Michaud EJ, Yoder BK. An Essential Role for Dermal Primary Cilia in Hair Follicle Morphogenesis. J.Invest.Dermatol. 2008 Nov 6.

Lei ZM, Mishra S, Zou W, Xu B, Foltz M, Li X, et al. Targeted disruption of luteinizing hormone/human chorionic gonadotropin receptor gene. Mol.Endocrinol. 2001 Jan;15(1):184-200.

Li YF, He W, Jha KN, Klotz K, Kim YH, Mandal A, et al. FSCB, a novel protein kinase A-phosphorylated calcium-binding protein, is a CABYR-binding partner involved in late steps of fibrous sheath biogenesis. J.Biol.Chem. 2007 Nov 23;282(47):34104-19.

Lin L, Faraco J, Li R, Kadotani H, Rogers W, Lin X, et al. The sleep disorder canine narcolepsy is caused by a mutation in the hypocretin (orexin) receptor 2 gene. Cell 1999 Aug 6;98(3):365-76.

Linford E, Glover FA, Bishop C, Stewart DL. The relationship between semen evaluation methods and fertility in the bull. J.Reprod.Fertil. 1976 Jul;47(2):283-91.

Loges NT, Olbrich H, Fenske L, Mussaffi H, Horvath J, Fliegauf M, et al. DNAI2 mutations cause primary ciliary dyskinesia with defects in the outer dynein arm. Am.J.Hum.Genet. 2008 Nov;83(5):547-58.

Lunenfeld B IV. Infertility: The dimension of the Problem. 1993;In Infertility Male and Female(2nd ed.).

Lupin AJ, Misko GJ. Kartagener syndrome with abnormalities of cilia. J.Otolaryngol. 1978 Apr;7(2):95-102.

Maatouk DM, Loveland KL, McManus MT, Moore K, Harfe BD. Dicer1 is required for differentiation of the mouse male germline. Biol.Reprod. 2008 Oct;79(4):696-703.

Maqsood M. An abnormality of mammalian spermatozoa. Experientia 1951 Aug 15;7(8):304.

Mendis-Handagama SM. Luteinizing hormone on Leydig cell structure and function. Histol. Histopathol. 1997 Jul;12(3):869-82.

Miki K. Energy metabolism and sperm function. Soc.Reprod.Fertil.Suppl. 2007;65:309-25.

Miki K, Qu W, Goulding EH, Willis WD, Bunch DO, Strader LF, et al. Glyceraldehyde 3-phosphate dehydrogenase-S, a sperm-specific glycolytic enzyme, is required for sperm motility and male fertility. Proc.Natl.Acad.Sci.U.S.A. 2004 Nov 23;101(47):16501-6.

Mitchell BF, Pedersen LB, Feely M, Rosenbaum JL, Mitchell DR. ATP production in Chlamydomonas reinhardtii flagella by glycolytic enzymes. Mol. Biol.Cell 2005 Oct;16(10):4509-18.

Moore A, Escudier E, Roger G, Tamalet A, Pelosse B, Marlin S, et al. RPGR is mutated in patients with a complex X linked phenotype combining primary ciliary dyskinesia and retinitis pigmentosa. J.Med.Genet. 2006 Apr;43(4):326-33.

Mruk DD, Cheng CY. Sertoli-Sertoli and Sertoli-germ cell interactions and their significance in germ cell movement in the seminiferous epithelium during spermatogenesis. Endocr.Rev. 2004 Oct;25(5):747-806.

Mulhardt C, Fischer M, Gass P, Simon-Chazottes D, Guenet JL, Kuhse J, et al. The spastic mouse: aberrant splicing of glycine receptor beta subunit mRNA caused by intronic insertion of L1 element. Neuron 1994 Oct;13(4):1003-15.

Naaby-Hansen S, Mandal A, Wolkowicz MJ, Sen B, Westbrook VA, Shetty J, et al. CABYR, a novel calcium-binding tyrosine phosphorylation-regulated fibrous sheath protein involved in capacitation. Dev.Biol. 2002 Feb 15;242(2):236-54.

Nakamura K, Iitsuka K, Fujii T. Adenylate kinase is tightly bound to axonemes of Tetrahymena cilia. Comp.Biochem.Physiol.B.Biochem.Mol.Biol. 1999 Oct;124(2):195-9.

Namekawa SH, Park PJ, Zhang LF, Shima JE, McCarrey JR, Griswold MD, et al. Postmeiotic sex chromatin in the male germline of mice. Curr.Biol. 2006 Apr 4;16(7):660-7.

Nantel F, Monaco L, Foulkes NS, Masquilier D, LeMeur M, Henriksen K, et al. Spermiogenesis deficiency and germ-cell apoptosis in CREM-mutant mice. Nature 1996 Mar 14;380(6570):159-62.

Narisawa S, Hecht NB, Goldberg E, Boatright KM, Reed JC, Millan JL. Testis-specific cytochrome c-null mice produce functional sperm but undergo early testicular atrophy. Mol.Cell.Biol. 2002 Aug;22(15):5554-62.

Neugebauer DC, Neuwinger J, Jockenhovel F, Nieschlag E. '9 + 0' axoneme in spermatozoa and some nasal cilia of a patient with totally immotile spermatozoa associated with thickened sheath and short midpiece. Hum.Reprod. 1990 Nov;5(8):981-6.

Nigumann P, Redik K, Matlik K, Speek M. Many human genes are transcribed from the antisense promoter of L1 retrotransposon. Genomics 2002 May;79(5):628-34.

Oakberg EF. Duration of spermatogenesis in the mouse. Nature 1957 Nov 23;180(4595):1137-8.

Okada H, Fujioka H, Tatsumi N, Fujisawa M, Gohji K, Arakawa S, et al. Assisted reproduction for infertile patients with 9 + 0 immotile spermatozoa associated with autosomal dominant polycystic kidney disease. Hum.Reprod. 1999 Jan;14(1):110-3.

Oko R, Clermont Y. Light microscopic immunocytochemical study of fibrous sheath and outer dense fiber formation in the rat spermatid. Anat.Rec. 1989 Sep;225(1):46-55.

Olbrich H, Haffner K, Kispert A, Volkel A, Volz A, Sasmaz G, et al. Mutations in DNAH5 cause primary ciliary dyskinesia and randomization of left-right asymmetry. Nat.Genet. 2002 Feb;30(2):143-4.

Omoto CK, Gibbons IR, Kamiya R, Shingyoji C, Takahashi K, Witman GB. Rotation of the central pair microtubules in eukaryotic flagella. Mol. Biol.Cell 1999 Jan;10(1):1-4.

Omoto CK, Yagi T, Kurimoto E, Kamiya R. Ability of paralyzed flagella mutants of Chlamydomonas to move. Cell Motil.Cytoskeleton 1996;33(2):88-94.

Omran H, Kobayashi D, Olbrich H, Tsukahara T, Loges NT, Hagiwara H, et al. Ktu/PF13 is required for cytoplasmic pre-assembly of axonemal dyneins. Nature 2008 Dec 4;456(7222):611-6.

O'Shaughnessy PJ, Hu L, Baker PJ. Effect of germ cell depletion on levels of specific mRNA transcripts in mouse Sertoli cells and Leydig cells. Reproduction 2008 Jun;135(6):839-50.

Ostrowski LE, Andrews K, Potdar P, Matsuura H, Jetten A, Nettesheim P. Cloning and characterization of KPL2, a novel gene induced during ciliogenesis of tracheal epithelial cells. Am.J.Respir.Cell Mol.Biol. 1999 Apr;20(4):675-83.

Pan J, Wang Q, Snell WJ. Cilium-generated signaling and cilia-related disorders. Lab.Invest. 2005 Apr;85(4):452-63.

Pazour GJ, Rosenbaum JL. Intraflagellar transport and cilia-dependent diseases. Trends Cell Biol. 2002 Dec;12(12):551-5.

Pazour GJ, Witman GB. Forward and reverse genetic analysis of microtubule motors in Chlamydomonas. Methods 2000 Dec;22(4):285-98.

Pennarun G, Escudier E, Chapelin C, Bridoux AM, Cacheux V, Roger G, et al. Loss-of-function mutations in a human gene related to Chlamydomonas reinhardtii dynein IC78 result

in primary ciliary dyskinesia. Am.J.Hum.Genet. 1999 Dec;65(6):1508-19.

Petersen C, Aumuller G, Bahrami M, Hoyer-Fender S. Molecular cloning of Odf3 encoding a novel coiled-coil protein of sperm tail outer dense fibers. Mol.Reprod.Dev. 2002 Jan;61(1):102-12.

Petersen C, Soder O. The sertoli cell--a hormonal target and 'super' nurse for germ cells that determines testicular size. Horm.Res. 2006;66(4):153-61.

Porter ME, Sale WS. The 9 + 2 axoneme anchors multiple inner arm dyneins and a network of kinases and phosphatases that control motility. J.Cell Biol. 2000 Nov 27;151(5):F37-42.

Pullen TJ, Ginger ML, Gaskell SJ, Gull K. Protein targeting of an unusual, evolutionarily conserved adenylate kinase to a eukaryotic flagellum. Mol. Biol.Cell 2004 Jul;15(7):3257-65.

Rannikki AS, Zhang FP, Huhtaniemi IT. Ontogeny of follicle-stimulating hormone receptor gene expression in the rat testis and ovary. Mol.Cell. Endocrinol. 1995 Feb;107(2):199-208.

Rawe VY, Galaverna GD, Acosta AA, Olmedo SB, Chemes HE. Incidence of tail structure distortions associated with dysplasia of the fibrous sheath in human spermatozoa. Hum.Reprod. 2001 May;16(5):879-86.

Rivkin E, Cullinan EB, Tres LL, Kierszenbaum AL. A protein associated with the manchette during rat spermiogenesis is encoded by a gene of the TBP-1-like subfamily with highly conserved ATPase and protease domains. Mol.Reprod.Dev. 1997 Sep;48(1):77-89.

Roberts SJ. Infertility in male animals. 1986;Woodstock(SJ Roberts).

Ruiz-Pesini E, Diez-Sanchez C, Lopez-Perez MJ, Enriquez JA. The role of the mitochondrion in sperm function: is there a place for oxidative phosphorylation or is this a purely glycolytic process? Curr.Top.Dev.Biol. 2007;77:3-19.

Rupp G, O'Toole E, Gardner LC, Mitchell BF, Porter ME. The sup-pf-2 mutations of Chlamydomonas alter the activity of the outer dynein arms by modification of the gamma-dynein heavy chain. J.Cell Biol. 1996 Dec;135(6 Pt 2):1853-65.

Russel L.D., Ettlin R. A., Sinha H.A.P. and Legg E. D. Mammalian spermatogenesis. In: Histological and histopathological evaluation of the testis. Clearwater, FL: Cache River Press; 1990.

Sapiro R, Kostetskii I, Olds-Clarke P, Gerton GL, Radice GL, Strauss III JF. Male infertility, impaired sperm motility, and hydrocephalus in mice deficient in sperm-associated antigen 6. Mol.Cell.Biol. 2002 Sep;22(17):6298-305.

Satir P, Christensen ST. Structure and function of mammalian cilia. Histochem.Cell Biol. 2008 Jun;129(6):687-93.

Scholey JM, Anderson KV. Intraflagellar transport and cilium-based signaling. Cell 2006 May 5;125(3):439-42.

Schultz N, Hamra FK, Garbers DL. A multitude of genes expressed solely in meiotic or postmeiotic spermatogenic cells offers a myriad of contraceptive targets. Proc.Natl.Acad.Sci.U.S.A. 2003 Oct 14;100(21):12201-6.

Severynse DM, Hutchison CA,3rd, Edgell MH. Identification of transcriptional regulatory activity within the 5' A-type monomer sequence of the mouse LINE-1 retroposon. Mamm. Genome 1992;2(1):41-50.

Shao X, Tarnasky HA, Lee JP, Oko R, van der Hoorn FA. Spag4, a novel sperm protein, binds outer dense-fiber protein Odf1 and localizes to microtubules of manchette and axoneme. Dev. Biol. 1999 Jul 1;211(1):109-23.

Shao X, Tarnasky HA, Schalles U, Oko R, van der Hoorn FA. Interactional cloning of the 84-kDa major outer dense fiber protein Odf84. Leucine zippers mediate associations of Odf84 and Odf27. J.Biol.Chem. 1997 Mar 7;272(10):6105-13.

Shao X, Xue J, van der Hoorn FA. Testicular protein Spag5 has similarity to mitotic spindle protein Deepest and binds outer dense fiber protein Odf1. Mol.Reprod.Dev. 2001 Aug;59(4):410-6.

Shapiro J, Ingram J, Johnson KA. Characterization of a molecular chaperone present in the eukaryotic flagellum. Eukaryot.Cell. 2005 Sep;4(9):1591-4.

Shima JE, McLean DJ, McCarrey JR, Griswold MD. The murine testicular transcriptome: characterizing gene expression in the testis during the progression of spermatogenesis. Biol. Reprod. 2004 Jul;71(1):319-30.

Silflow CD, Lefebvre PA. Assembly and motility of eukaryotic cilia and flagella. Lessons from Chlamydomonas reinhardtii. Plant Physiol. 2001 Dec;127(4):1500-7.

Smith EF, Lefebvre PA. The role of central apparatus components in flagellar motility and microtubule assembly. Cell Motil.Cytoskeleton 1997;38(1):1-8.

Steels JD, Estey MP, Froese CD, Reynaud D, Pace-Asciak C, Trimble WS. Sept12 is a component of the mammalian sperm tail annulus. Cell Motil. Cytoskeleton 2007 Oct;64(10):794-807.

Steger K. Transcriptional and translational regulation of gene expression in haploid spermatids. Anat. Embryol.(Berl) 1999 Jun;199(6):471-87.

Sukura A, Mäkipää R, Vierula M, Rodriguez-Martinez H, Sundback P, Andersson M. Hereditary sterilizing short-tail sperm defect in Finnish Yorkshire boars. J.Vet.Diagn.Invest. 2002 Sep;14(5):382-8.

Sullivan R. Male fertility markers, myth or reality. Anim.Reprod.Sci. 2004 Jul;82-83:341-7.

Suzuki-Toyota F, Ito C, Toyama Y, Maekawa M, Yao R, Noda T, et al. The coiled tail of the round-headed spermatozoa appears during epididymal passage in GOPC-deficient mice. Arch.Histol. Cytol. 2004 Nov;67(4):361-71.

Tanaka H, Baba T. Gene expression in spermiogenesis. Cell Mol.Life Sci. 2005 Feb;62(3):344-54.

Travis AJ, Foster JA, Rosenbaum NA, Visconti PE, Gerton GL, Kopf GS, et al. Targeting of a germ cell-specific type 1 hexokinase lacking a porin-binding domain to the mitochondria as well as to the head and fibrous sheath of murine spermatozoa. Mol.Biol.Cell 1998 Feb;9(2):263-76.

Tres LL, Kierszenbaum AL. Sak57, an acidic keratin initially present in the spermatid manchette before becoming a component of paraaxonemal structures of the developing tail. Mol.Reprod. Dev. 1996 Jul;44(3):395-407.

Turner RM. Moving to the beat: a review of mammalian sperm motility regulation. Reprod. Fertil.Dev. 2006;18(1-2):25-38.

Turner RM. Tales from the tail: what do we really know about sperm motility? J.Androl. 2003 Nov-Dec;24(6):790-803.

Van's Gravesande KS, Omran H. Primary ciliary dyskinesia: clinical presentation, diagnosis and genetics. Ann.Med. 2005;37(6):439-49.

Ventela S, Toppari J, Parvinen M. Intercellular organelle traffic through cytoplasmic bridges in early spermatids of the rat: mechanisms of haploid gene product sharing. Mol.Biol.Cell 2003 Jul;14(7):2768-80.

Vidal F, Lopez P, Lopez-Fernandez LA, Ranc F, Scimeca JC, Cuzin F, et al. Gene trap analysis of germ cell signaling to Sertoli cells: NGF-TrkA mediated induction of Fra1 and Fos by post-meiotic germ cells. J.Cell.Sci. 2001 Jan;114(Pt 2):435-43.

Vierula M, Alanko M, Remes E, Vanha-Perttula T. Ultrastructure of a tail stump sperm defect in an Ayrshire bull. Andrologia 1983 Jul-Aug;15(4):303-9.

Wallace MS. Infertility in the male dog. Probl.Vet. Med. 1992 Sep;4(3):531-44.

Wargo MJ, Smith EF. Asymmetry of the central apparatus defines the location of active microtubule sliding in Chlamydomonas flagella. Proc.Natl.Acad.Sci.U.S.A. 2003 Jan 7;100(1):137-42.

Welch JE, Brown PL, O'Brien DA, Magyar PL, Bunch DO, Mori C, et al. Human glyceraldehyde 3-phosphate dehydrogenase-2 gene is expressed specifically in spermatogenic cells. J.Androl. 2000 Mar-Apr;21(2):328-38.

Whitfield JF. The neuronal primary cilium--an extrasynaptic signaling device. Cell.Signal. 2004 Jul;16(7):763-7.

Wirschell M, Pazour G, Yoda A, Hirono M, Kamiya R, Witman GB. Oda5p, a novel axonemal protein required for assembly of the outer dynein arm and an associated adenylate kinase. Mol.Biol. Cell 2004 Jun;15(6):2729-41.

Yagi T, Minoura I, Fujiwara A, Saito R, Yasunaga T, Hirono M, et al. An axonemal dynein particularly important for flagellar movement at high viscosity. Implications from a new Chlamydomonas mutant deficient in the dynein heavy chain gene DHC9. J.Biol.Chem. 2005 Dec 16;280(50):41412-20.

Yoshida T, Ioshii SO, Imanaka-Yoshida K, Izutsu K. Association of cytoplasmic dynein with manchette microtubules and spermatid nuclear envelope during spermiogenesis in rats. J.Cell. Sci. 1994 Mar;107 (Pt 3)(Pt 3):625-33.

Yoshida T, Takanari H, Izutsu K. Distribution of cytoplasmic and axonemal dyneins in rat tissues. J.Cell.Sci. 1992 Mar;101 (Pt 3)(Pt 3):579-87.

Zariwala MA, Knowles MR, Omran H. Genetic defects in ciliary structure and function. Annu. Rev.Physiol. 2007;69:423-50.

Zarsky HA, Tarnasky HA, Cheng M, van der Hoorn FA. Novel RING finger protein OIP1 binds to conserved amino acid repeats in sperm tail protein ODF1. Biol.Reprod. 2003 Feb;68(2):543-52.

Zhang H, Mitchell DR. Cpc1, a Chlamydomonas central pair protein with an adenylate kinase domain. J.Cell.Sci. 2004 Aug 15;117(Pt 18):4179-88.

Zhang Z, Kostetskii I, Moss SB, Jones BH, Ho C, Wang H, et al. Haploinsufficiency for the murine orthologue of Chlamydomonas PF20 disrupts spermatogenesis. Proc.Natl.Acad.Sci.U.S.A. 2004 Aug 31;101(35):12946-51.